

Metal Chelation-Controlled Twisted Intramolecular Charge Transfer and Its Application to Fluorescent Sensing of Metal Ions and Anions

Shin Aoki,^{*,†} Daisuke Kagata,[‡] Motoo Shiro,[§] Kei Takeda,[‡] and Eiichi Kimura^{*,#}

Contribution from the Faculty of Pharmaceutical Sciences, Tokyo University of Science, 2641 Yamazaki, Noda, Chiba 278-8510, Japan, Division of Medicinal Chemistry, Graduate School of Biomedical Sciences, Hiroshima University, 1-2-3 Kasumi, Minami-ku, Hiroshima 734-8551, Japan, Rigaku Corporation X-ray Research Laboratory, 3-9-12 Matsubaracho, Akishima, Tokyo 196-8666, Japan, and Faculty of Integrated Arts and Sciences, Hiroshima University, 1-7-1 Kagamiyama, Higashi-Hiroshima 739-8521, Japan

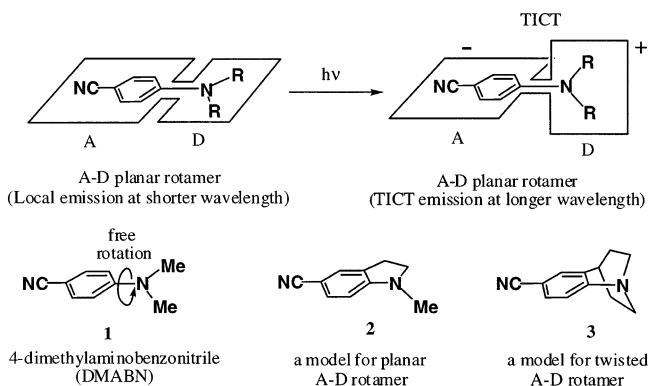
Received April 1, 2004; E-mail: shinaoki@rs.noda.tus.ac.jp; ekimura@hiroshima-u.ac.jp

Abstract: Two fluorescent ligands, *N*-(2-(5-cyanopyridyl))cyclen (L5) and *N*-(2-pyridyl)cyclen (L6) (cyclen = 1,4,7,10-tetraazacyclododecane), were designed and synthesized to control twisted intramolecular charge transfer (TICT) by metal chelation in aqueous solution. By complexation with Zn²⁺, L6 exhibited TICT emissions at 430 nm (excitation at 270 nm) in 10 mM HEPES (pH 7.0) with *I* = 0.1 (NaNO₃) at 25 °C due to the perpendicular conformation of a pyridine ring with respect to a dialkylamino group, which was fixed by Zn²⁺–N(pyridine) coordination, as proven by potentiometric pH, UV, and fluorescence titrations and X-ray crystal structure analysis. We further describe that the 1:1 complexation of ZnL6 with guests such as succinimide, phosphates, thiolates, and dicarboxylates, which compete with a nitrogen in the pyridine ring for Zn²⁺ in ZnL6, induces considerable emission shift from TICT emissions (at 430 nm) to locally excited emissions (at ca. 350 nm) in neutral aqueous solution at 25 °C.

Introduction

Dual fluorescence emissions of 4-(*N,N*-dimethylamino)-benzonitrile (DMABN, **1**) were first observed by Lippert et al. about 40 years ago.^{1,2} An emission of **1** at shorter wavelengths (~330 nm), which occurs in less polar solvents, has been ascribed to locally excited (LE) states. In contrast, an anomalous emission at longer wavelengths (420–460 nm) in polar solvents is currently accounted for by the concept of twisted intramolecular charge transfer (TICT),^{3,4} in which the emission of **1** is attributed to a charge separation in an orthogonal rotamer with respect to a C–N linkage between an acceptor (A) group (phenyl ring) and a donor (D) group (dimethylamino group) in the excited states (Scheme 1). In support of the TICT theory,

Scheme 1



[†] Tokyo University of Science.

[‡] Graduate School of Biomedical Sciences, Hiroshima University.

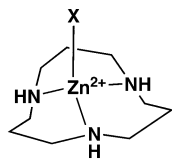
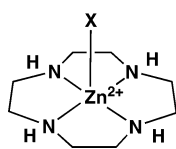
[§] Rigaku Corp.

[#] Faculty of Integrated Arts and Sciences, Hiroshima University.

- (1) (a) Lippert, E.; Lüder, W.; Moll, F.; Nagele, H.; Boos, H.; Prigge, H.; Siebold-Blankenstein, I. *Angew. Chem.* **1961**, *73*, 695–706. (b) Lippert, E.; Lüder, W.; Boos, H. In *Advances in Molecular Spectroscopy*; Mangini, A., Ed.; Pergamon Press: Oxford, 1962; Vol. 1, pp 443–457.
- (2) Rettig, W.; Maus, M. In *Conformational Analysis of Molecules in Excited States*; Waluk, J., Ed.; Wiley-VCH: New York, 2000; pp 1–5.
- (3) (a) Rotkiewica, K.; Grellman, K. H.; Grabowski, Z. R. *Chem. Phys. Lett.* **1973**, *19*, 315–318. (b) Grabowski, Z. R.; Rotkiewicz, K.; Siemiarczuk, A. *J. Lumin.* **1979**, *18/19*, 420–424. (c) Grabowski, Z. R.; Rotkiewicz, K.; Siemiarczuk, A.; Cowley, D. J.; Baumann, W. *Nouv. J. Chim.* **1979**, *3*, 443–454.
- (4) (a) Rettig, W. *Angew. Chem., Int. Ed. Engl.* **1986**, *25*, 971–988. (b) Rettig, W.; Lippert, E. *J. Mol. Struct.* **1980**, *61*, 17–22. (c) Rettig, W.; Baumann, W. In *Progress in Photochemistry and Photophysics*; Rabek, J. F., Ed.; CRC Press: Boca Raton, FL, 1990; Vol. 6, pp 79–134. (d) Klessinger, M.; Michl, J. *Excited States and Photochemistry of Organic Molecules*; VCH Publishers: New York, 1995.

compound **2**, in which the A–D linkage is fixed to be planar, emits only short-wavelength fluorescence. In contrast, an A–D twisted model compound **3** exhibits only an anomalous emission at a longer wavelength. Although many experimental and theoretical studies have been performed, the TICT theory is still controversial and metal chelation control of TICT has remained elusive.^{5,6}

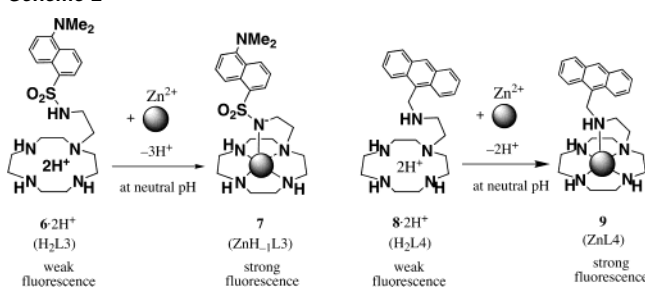
Macrocyclic polyamines have been proven to be versatile metal chelators in aqueous solution.^{7,8} Zn²⁺ complexes such as Zn²⁺–[12]aneN₃ (ZnL1, **4**)⁹ and Zn²⁺–cyclen (ZnL2, **5**),¹⁰ are stable in aqueous solution at neutral pH (cyclen = 1,4,7,10-tetraazacyclododecane) and are good models for zinc(II) enzymes such as carbonic anhydrase,⁹ alkaline phosphatase,¹⁰ β-lactamase,¹¹ and type II (Zn²⁺-dependent) aldolase.¹² Fur-

Zn²⁺-[12]aneN₃ (ZnL1)Zn²⁺-cyclen (ZnL2)4a: X = OH₂ (pK_a = 7.30)4b: X = OH⁻5a: X = OH₂ (pK_a = 7.86)5b: X = OH⁻

thermore, these Zn²⁺ complexes are good receptors of various anions, including carboxylates,^{10,13} phosphates,^{10,14} imides (such as thymine),^{15,16} and thiolates.^{11,17}

We have also been interested in the photochemical properties of macrocyclic polyamines bearing photoresponsive moieties.^{18–23} For example, a Zn²⁺ fluorophore, dansylethylamide cyclen **6** (L3), quantitatively responds to Zn²⁺ at submicromolar concentrations in neutral aqueous solution (L3 exists as a diprotonated form, H₂L3, at neutral pH) due to a coordination of deprotonated dansylamide N⁻ to Zn²⁺, yielding a complex **7**

Scheme 2



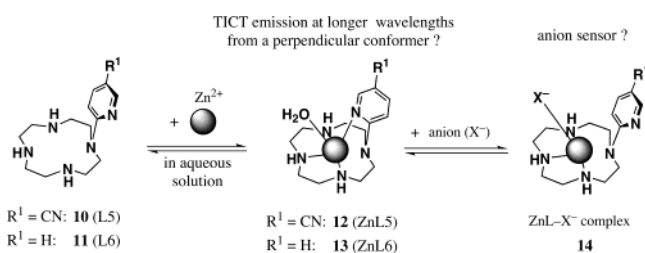
(Zn(H₋₁L3)) (Scheme 2).^{18,19} In addition, it has been discovered that **6** (L3) selectively stains apoptotic cells at their early stages.²⁰ To improve the selectivity and sensitivity of Zn²⁺, 2-(9-anthrylmethylamino)ethylcyclen **8** (L4) has been synthesized.²¹ The emission enhancement in the 1:1 Zn²⁺-L4 complex **9** is due to the retardation of photoinduced electron transfer (PET) by the chelation of a nitrogen atom of the side chain to Zn²⁺. However, only a slight emission shift was observed for **6** and **8** upon complexation with Zn²⁺, which might be a drawback in the quantification of Zn²⁺ concentration in living cells.^{24,25}

On the basis of these results, we have designed and synthesized two ligands, *N*-(2-(5-cyanopyridyl)cyclen) **10** (L5) and *N*-(2-pyridyl)cyclen **11** (L6). We hypothesized that the pyridine moieties of L5 and L6 could chelate to metal cations such as Zn²⁺, so that the conformation of a pyridine ring would be fixed perpendicular to a dialkylamino group, resulting in an emission at longer wavelengths due to TICT (Scheme 3). Herein,

- (5) For recent discussions, see: (a) Köhler, G.; Rechthaler, K.; Grabner, G.; Luboradzki, R.; Suwinska, K.; Rotkiewica, K. *J. Phys. Chem. A* **1997**, *101*, 8518–8525. (b) Dreyer, J.; Kummrow, A. *J. Am. Chem. Soc.* **2000**, *122*, 2577–2585. (c) Demeter, A.; Druzhinin, S.; George, M.; Haselbach, E.; Roulin, J.-L.; Zachariasse, K. A. *Chem. Phys. Lett.* **2000**, *323*, 351–360. (d) Kwok, W. M.; Ma, C.; Phillips, D.; Matousek, P.; Parker, A. W.; Towrie, M. *J. Phys. Chem. A* **2000**, *104*, 4188–4197. (e) Mennucci, B.; Toniolo, A.; Tomasi, J. *J. Am. Chem. Soc.* **2000**, *122*, 10621–10630. (f) Mishina, S.; Takayanagi, M.; Nakata, M.; Otsuki, J.; Araki, K. *J. Photochem. Photobiol. A* **2001**, *141*, 153–158. (g) Dobkowski, J.; Wójcik, J.; Kózmński, W.; Kolos, R.; Waluk, J.; Michl, J. *J. Am. Chem. Soc.* **2002**, *124*, 2406–2407.
- (6) For several attempts to control TICT in host–guest complex systems, see: (a) Hamasaki, K.; Ikeda, H.; Nakamura, A.; Ueno, A.; Toda, F.; Suzuki, I.; Osa, T. *J. Am. Chem. Soc.* **1993**, *115*, 5035–5040. (b) Létard, J.-F.; Delmond, S.; Lapouyade, R.; Braun, D.; Rettig, W.; Kreissler, M. *Recl. Trav. Chim. Pays-Bas* **1995**, *114*, 517–527. (c) Kundu, S.; Chattopadhyay, N. *J. Mol. Struct.* **1995**, *344*, 151–155. (d) Choi, L.-S.; Collins, G. E. *J. Chem. Soc., Chem. Commun.* **1998**, 893–894. (e) Collins, G. E.; Choi, L.-S.; Callahan, J. H. *J. Am. Chem. Soc.* **1998**, *120*, 1474–1478. (f) Krishnamoorthy, G.; Dogra, S. K. *J. Phys. Chem. A* **2000**, *104*, 2542–2551. (g) Morozumi, T.; Anada, T.; Nakamura, H. *J. Phys. Chem. B* **2001**, *105*, 2923–2931.
- (7) Martell, A. E.; Hancock, R. D. *Metal Complexes in Aqueous Solutions*; Plenum Press: New York, 1996.
- (8) (a) Kimura, E.; Koike, T.; Shionoya, M. In *Structure and Bonding: Metal Site in Proteins and Models*; Sadler, J. P., Ed.; Springer: Berlin, 1997; Vol. 89, pp 1–28. (b) Kimura, E.; Koike, T. In *Comprehensive Supramolecular Chemistry*; Reinhoudt, D. N., Ed.; Pergamon: Tokyo, 1996; Vol. 10, pp 429–444. (c) Kimura, E.; Koike, T. *J. Chem. Soc., Chem. Commun.* **1998**, 1495–1500. (d) Kimura, E.; Koike, T. In *Bioinorganic Catalysis*; Reedijk, J.; Bouwman, E., Eds.; Marcel Dekker, Inc.: New York, 1999; pp 33–54. (e) Kimura, E.; Kikuta, E. *J. Biol. Inorg. Chem.* **2000**, *5*, 139–155. (f) Kimura, E. *Curr. Opin. Chem. Biol.* **2000**, *4*, 207–213. (g) Kimura, E. *Acc. Chem. Res.* **2001**, *34*, 171–179. (h) Aoki, S.; Kimura, E. In *Comprehensive Coordination Chemistry II*; Que, L., Jr., Tolman, W. B., Eds.; Elsevier Ltd.: Amsterdam, 2004; Vol. 8, pp 601–640. (i) Aoki, S.; Kimura, E. *Chem. Rev.* **2004**, *104*, 769–787.
- (9) (a) Kimura, E.; Shiota, T.; Koike, T.; Shiro, M.; Kodama, M. *J. Am. Chem. Soc.* **1990**, *112*, 5805–5811. (b) Koike, T.; Kimura, E.; Nakamura, I.; Hashimoto, Y.; Shiro, M. *J. Am. Chem. Soc.* **1992**, *114*, 7338–7345. (c) Zhang, X.; van Eldik, R.; Koike, T.; Kimura, E. *Inorg. Chem.* **1993**, *32*, 5749–5755.
- (10) (a) Koike, T.; Kimura, E. *J. Am. Chem. Soc.* **1991**, *113*, 8935–8941. (b) Kimura, E.; Nakamura, I.; Koike, T.; Shionoya, M.; Kodama, Y.; Ikeda, T.; Shiro, M. *J. Am. Chem. Soc.* **1994**, *116*, 4764–4771. (c) Koike, T.; Kajitani, S.; Nakamura, I.; Kimura, E.; Shiro, M. *J. Am. Chem. Soc.* **1995**, *117*, 1210–1219. (d) Kimura, E.; Kodama, Y.; Koike, T.; Shiro, M. *J. Am. Chem. Soc.* **1995**, *117*, 8304–8311.
- (11) Koike, T.; Takamura, M.; Kimura, E. *J. Am. Chem. Soc.* **1994**, *116*, 8443–8449.
- (12) Kimura, E.; Gotoh, T.; Aoki, S.; Kimura, E. *J. Am. Chem. Soc.* **1999**, *121*, 6730–6737.
- (13) Kimura, E.; Ikeda, T.; Shionoya, M.; Shiro, M. *Angew. Chem., Int. Ed. Engl.* **1995**, *34*, 663–664.
- (14) (a) Aoki, S.; Kimura, E. *Rev. Mol. Biotech.* **2002**, *90*, 129–155. (b) Kimura, E.; Aoki, S.; Koike, T.; Shiro, M. *J. Am. Chem. Soc.* **1997**, *119*, 3068–3076. (c) Aoki, S.; Kimura, E. *J. Am. Chem. Soc.* **2000**, *122*, 4542–4548. (d) Aoki, S.; Iwaida, K.; Hanamoto, N.; Shiro, M.; Kimura, E. *J. Am. Chem. Soc.* **2002**, *124*, 5256–5257.

- (15) (a) Shionoya, M.; Kimura, E.; Shiro, M. *J. Am. Chem. Soc.* **1993**, *115*, 12–6737. (b) Shionoya, M.; Kimura, E.; Hayashida, H.; Pettho, G.; Marzilli, L. G. *Supramol. Chem.* **1993**, *2*, 173–176. (c) Shionoya, M.; Ikeda, T.; Kimura, E.; Shiro, M. *J. Am. Chem. Soc.* **1994**, *116*, 3848–3859. (d) Kimura, E.; Ikeda, T.; Aoki, S.; Shionoya, M. *J. Biol. Inorg. Chem.* **1998**, *3*, 259–267. (e) Aoki, S.; Honda, Y.; Kimura, E. *J. Am. Chem. Soc.* **1998**, *120*, 10018–10026. (f) Aoki, S.; Sugimura, C.; Kimura, E. *J. Am. Chem. Soc.* **1998**, *120*, 10094–10102. (g) Kimura, E.; Kikuchi, M.; Kitamura, H.; Koike, T. *Chem. Eur. J.* **1999**, *5*, 3113–123. (h) Kikuta, E.; Murata, M.; Katsube, N.; Koike, T.; Kimura, E. *J. Am. Chem. Soc.* **1999**, *121*, 5426–5436. (i) Kimura, E.; Kikuta, E. *Prog. React. Kinet. Mech.* **2000**, *25*, 1–64. (j) Kimura, E.; Kitamura, H.; Ohtani, K.; Koike, T. *J. Am. Chem. Soc.* **2000**, *122*, 4668–4677. (k) Kikuta, E.; Aoki, S.; Kimura, E. *J. Am. Chem. Soc.* **2001**, *123*, 7911–7912. (l) Kikuta, E.; Aoki, S.; Kimura, E. *J. Biol. Inorg. Chem.* **2002**, *7*, 473–482. (m) Kimura, E.; Katsube, N.; Koike, T.; Shiro, M.; Aoki, S. *Supramol. Chem.* **2002**, *14*, 2002.
- (16) Aoki, S.; Koike, T.; Shiro, M.; Kimura, E. *J. Am. Chem. Soc.* **2000**, *122*, 576–584.
- (17) (a) Aoki, S.; Shiro, M.; Kimura, E. *Chem. Eur. J.* **2002**, *8*, 929–939. (b) Aoki, S.; Zulkefeli, M.; Shiro, M.; Kimura, E. *Proc. Natl. Acad. Sci. U.S.A.* **2002**, *99*, 4894–4899.
- (18) Kimura, E.; Aoki, S. *BioMetals* **2001**, *14*, 191–204.
- (19) (a) Koike, T.; Watanabe, T.; Aoki, S.; Kimura, E.; Shiro, M. *J. Am. Chem. Soc.* **1996**, *118*, 12696–12703. (b) Kimura, E. *S. Afr. J. Chem.* **1997**, *50*, 240–248. (c) Kimura, E.; Koike, T. *Chem. Soc. Rev.* **1998**, *27*, 179–184.
- (20) (a) Kimura, E.; Aoki, S.; Kikuta, E.; Koike, T. *Proc. Natl. Acad. Sci., U.S.A.* **2003**, *100*, 3731–3736. (b) Kimura, E.; Takasawa, R.; Tanuma, S.; Aoki, S. *Science STKE* **2004**, *7*.
- (21) Aoki, S.; Kaido, S.; Fujioka, H.; Kimura, E. *Inorg. Chem.* **2003**, *42*, 1023–1030.
- (22) Koike, T.; Gotoh, T.; Aoki, S.; Kimura, E.; Shiro, M. *Inorg. Chim. Acta* **1998**, *270*, 424–432.
- (23) Aoki, S.; Kawatani, H.; Goto, T.; Kimura, E.; Shiro, M. *J. Am. Chem. Soc.* **2001**, *123*, 1123–1132.
- (24) For reviews of fluorescent sensors for metal ion, see: (a) *Fluorescent Chemosensors for Ion and Molecule Recognition*; Czarnik, A. W., Ed.; American Chemical Society: Washington, DC, 1993. (b) Lehn, J.-M. *Supramolecular Chemistry*; VCH: Weinheim, 1995. (c) *Advances in Supramolecular Chemistry*, Vol. 4; Gokel, G. W., Ed.; JAI Press Inc.: Greenwich, CT, 1997. (d) Sessler, J. L.; Gale, P. A. *The Porphyrin Handbook*; Kadish, K. M., Smith, K. M., Guillard, R., Eds.; Academic Press: San Diego, CA, and Burlington, MA, 2000. (e) Czarnik, A. W. *Acc. Chem. Res.* **1994**, *27*, 302–308. (f) Czarnik, A. W. *Chem. Biol.* **1995**, *2*, 423–428. (g) *Supramolecular Chemistry of Anions*; Bianchi, A., Bowman-James, K., Garcia-Espana, E., Eds.; Wiley-VCH: New York, 1996. (h) Schmidtchen, F. P.; Berger, M. *Chem. Rev.* **1997**, *97*, 1609–1646. (i) Prasanna de Silva, A.; Gunaratne, H. Q. N.; Gunnlaugsson, T.; Huxley, A. J. M.; McCoy, C. P.; Rademacher, J. T.; Rice, T. E. *Chem. Rev.* **1997**, *97*, 1515–1566.

Scheme 3



we describe a Zn^{2+} chelation control of TICT in the Zn^{2+} complexes **12** (ZnL5) and **13** (ZnL6) in aqueous solution. We then describe a sensing of anions (X^-) based on the conformational change of the pyridine ring in the ZnL6–anion complexes **14** (ZnL6– X^-).

Experimental Section

General Information. All reagents and solvents purchased were at the highest commercial quality and used without further purification. Anhydrous acetonitrile and toluene were obtained by distillation from CaH_2 or $LiAlH_4$. All aqueous solutions were prepared using deionized and distilled water. Buffer solutions (CAPS, pH 11.0, 10.8, 10.4, 10.0; CHES, pH 9.0, 8.7, 8.5; EPPS, pH 8.0; HEPES, pH 7.5, 7.4, 7.0; MES, pH 6.5, 6.0, 5.5; 5.0; AcOH–AcONa, pH 4.0, 3.5; citric acid–sodium citrate, pH 3.0, 2.5, 2.0) were used and the ionic strengths of all were adjusted to 0.1 with $NaNO_3$. The following Good's buffer reagents (pK_a at 25 °C) were commercially available from Dojindo (Kumamoto, Japan): CAPS (3-(cyclohexylamino)propanesulfonic acid, $pK_a = 10.4$), CHES (2-(cyclohexylamino)ethanesulfonic acid, $pK_a = 9.5$), EPPS (3-(4-(2-hydroxyethyl)-1-piperazinyl)propanesulfonic acid, $pK_a = 8.0$), HEPES (*N*-(2-hydroxyethyl)piperazine-*N'*'-2-ethanesulfonic acid, $pK_a = 7.6$), and MES (2-morpholinoethanesulfonic acid, $pK_a = 6.2$). Melting points were measured on a Yanaco melting point apparatus and listed without correlation. IR spectra were recorded on a Horiba FTIR-710 spectrophotometer at room temperature. 1H (500 MHz) and ^{13}C (125 MHz) NMR spectra at 35 ± 0.1 °C were recorded on a JEOL Delta 500 spectrometer. 3-(Trimethylsilyl)propionic-2,2,3,3- d_4 acid sodium salt (TSP) in D_2O and tetramethylsilane (TMS) in $CDCl_3$ and CD_3CN were used as internal references for 1H and ^{13}C NMR measurements. The pD values in D_2O were corrected for a deuterium isotope effect using $pD = (pH\text{-meter reading}) + 0.40$. Elemental analyses were performed on a Perkin-Elmer CHN 2400 analyzer. Thin-layer (TLC) and silica gel column chromatographies were performed using a Merck 5554 (silica gel) TLC plate and Fuji Silysia Chemical FL-100D, respectively.

1-(2-(5-Cyano)-pyridyl)-4,7,10-tris(*tert*-butyloxycarbonyl)-1,4,7,10-tetraazacyclododecane (16). A mixture of 3Boc-cyclen **15** (2.5 g,

5.3 mmol), 14b 2-chloro-5-cyanopyridine (245 mg, 1.8 mmol), and K_2CO_3 (368 mg, 2.7 mmol) in 1,4-dioxane (15 mL) was stirred at 100 °C under an argon atmosphere for 9 days. After insoluble inorganic salts were filtered off, the filtrate was concentrated under reduced pressure. The remaining residue was purified by silica gel column chromatography (hexane/AcOEt) to yield **16** as colorless amorphous solids (0.67 g, 65% yield). IR (KBr): 2976, 2931, 2218, 1693, 1603, 1510, 1468, 1412, 1365, 1248, 1165, 777 cm^{-1} . 1H NMR ($CDCl_3/TMS$): δ 1.41 (s, 18H), 1.47 (s, 9H), 3.35–3.7 (m, 16H), 6.58 (d, 1H, $J = 8.7$ Hz), 7.57 (dd, 1H, $J = 8.7, 2.3$ Hz), 8.40 (d, 1H, $J = 2.3$ Hz). ^{13}C NMR ($CDCl_3/TMS$): δ 28.37, 28.51, 49.56, 50.12, 51.86, 80.25, 80.44, 96.13, 106.12, 118.79, 139.33, 152.66, 156.46, 159.22.

1-(2-(5-Cyano)-pyridyl)-1,4,7,10-tetraazacyclododecane Ditrifluoroacetic Acid Salt (10-2TFA). Trifluoroacetic acid (4.2 mL, 55 mmol) was added dropwise to a solution of **16** (0.63 g, 1.1 mmol) in CH_2Cl_2 (10 mL) at 0 °C, and the whole was stirred for 6 h at room temperature. The reaction mixture was concentrated under reduced pressure and azeotroped with toluene. The remaining powders were recrystallized from EtOH to give **10-2TFA** (L5-2TFA) as colorless prisms (0.30 g, 51% yield), mp 184–185 °C. IR (KBr): 3240, 2925, 2210, 1672, 1603, 1419, 1203, 1178, 1128, 721 cm^{-1} . 1H NMR (D_2O/TSP): δ 3.22–3.25 (m, 8H), 3.32–3.34 (m, 4H), 3.92–3.94 (m, 4H), 6.94 (d, 1H, $J = 9.2$ Hz, ArH), 7.95 (dd, 1H, $J = 9.2, 2.1$ Hz, ArH), 8.56 (d, 1H, $J = 2.1$ Hz, ArH). ^{13}C NMR (D_2O): δ 46.17, 47.39, 48.32, 51.10, 100.61, 110.86, 121.74, 143.85, 155.40, 163.15. Anal. Calcd for $C_{18}H_{24}N_6O_4F_6$: C, 43.03; H, 4.82; N, 16.73. Found: C, 43.05; H, 4.89; N, 16.58.

1-(2-Pyridyl)-4,7,10-tris(*tert*-butyloxycarbonyl)-1,4,7,10-tetraazacyclododecane (17).²⁶ A mixture of 3Boc-cyclen **15** (3.5 g, 7.3 mmol), 14b 2-bromopyridine (1.6 g, 7.3 mmol), $Pd(OAc)_2$ (82 mg, 0.37 mmol), triphenylphosphine (192 mg, 0.73 mmol), and $NaOtBu$ (920 mg, 9.5 mmol) in toluene (10 mL) was stirred at 80 °C under an argon atmosphere for 2 days. The reaction mixture was diluted with CH_2Cl_2 and filtered through Celite (No. 545), and the filtrate was concentrated under reduced pressure. The remaining residue was purified by silica gel column chromatography (hexane/AcOEt) to yield **17** as colorless amorphous solids (2.3 g, 57% yield). IR (IR card): 2969, 1689, 1595, 1471, 1365, 1141, 774 cm^{-1} . 1H NMR ($CDCl_3/TMS$): δ 1.45 (s, 27H), 3.22 (brs, 4H), 3.43–3.51 (m, 8H), 3.67 (brs, 4H), 6.54–6.59 (m, 2H), 7.38–7.41 (m, 1H), 8.13, (dd, 1H, $J = 4.9, 1.3$ Hz). ^{13}C NMR ($CDCl_3$): δ 28.46, 28.54, 50.31, 50.61, 51.81, 79.87, 107.75, 112.45, 137.05, 147.76, 156.52, 159.53.

1-(2-Pyridyl)-1,4,7,10-tetraazacyclododecane-3HCl Salt (11-3HCl-1.5H₂O). Aqueous HCl (20%) (5 mL) was added dropwise to a solution of **17** (2.3 g, 4.2 mmol) in ethanol (15 mL) at 0 °C, and the whole was stirred overnight at room temperature. After the reaction mixture was concentrated under reduced pressure, the remaining powders were recrystallized from EtOH/ H_2O to give **11-3HCl-1.5H₂O** (11-3HCl-1.5H₂O) as colorless prisms (1.3 g, 79% yield), mp 202–204 °C. IR (KBr): 3410, 2952, 1638, 1606, 1537, 1419, 1272, 1181, 1001, 775, 544 cm^{-1} . 1H NMR (D_2O/TSP): δ 3.26–3.31 (m, 8H), 3.40–3.42 (m, 4H), 3.95–3.97 (m, 4H), 7.14 (dd, 1H, $J = 7.2, 6.7$ Hz), 7.25 (d, 1H, $J = 9.2$ Hz), 8.05–8.10 (m, 2H). ^{13}C NMR (D_2O): δ 47.38, 47.73, 48.95, 53.02, 116.02, 117.21, 139.38, 148.09, 155.17. Anal. Calcd for $C_{13}H_{29}N_3O_{1.5}Cl_3$: C, 40.48; H, 7.58; N, 18.15. Found: C, 40.29; H, 7.46; N, 18.02.

1-(2-Pyridyl)-1,4,7,10-tetraazacyclododecane–Zn(NO₃)₂ Complex, 13(NO₃)₂ (ZnL6(NO₃)₂). An aqueous solution of **11-3HCl-1.5H₂O** (1.0 g, 2.7 mmol) was added to a 5 N aqueous NaOH solution, and the solution was extracted with $CHCl_3$ (50 mL \times 5). After the combined organic layers were dried over anhydrous Na_2SO_4 , the solvent was concentrated under reduced pressure to obtain the free ligand **11** as a colorless oil. The free ligand **11** was dissolved in EtOH (10 mL), to which a solution of $Zn(NO_3)_2 \cdot 6H_2O$ (0.88 g, 3.0 mmol) in EtOH (10 mL) was added at 50 °C, and the whole was stirred for 1 h. After the

(25) For recent examples of fluorescent chemical sensors for Zn^{2+} , see: (a) Walkup, G. K.; Burdette, S. C.; Lippard, S. J.; Tsien, R. Y. *J. Am. Chem. Soc.* **2000**, *122*, 5644–5655. (b) Burdette, S. C.; Walkup, G. K.; Spingler, B.; Tsien, R. Y.; Lippard, S. J. *J. Am. Chem. Soc.* **2001**, *123*, 7831–7841. (c) Hirano, T.; Kikuchi, K.; Urano, Y.; Higuchi, T.; Nagano, T. *Angew. Chem., Int. Ed.* **2000**, *39*, 1052–1054. (d) Reany, O.; Gunnlaugsson, T.; Parker, D. J. *Chem. Soc., Chem. Commun.* **2000**, 473–474. (e) Pearce, D. A.; Jotterand, N.; Carrico, I. S.; Imperiali, B. *J. Am. Chem. Soc.* **2001**, *123*, 5160–5161. (f) Marvin, J. S.; Hellnga, H. W. *Proc. Natl. Acad. Sci., U.S.A.* **2001**, *98*, 4955–4960. (g) Bronwon, R. T.; Bradshaw, J. S.; Savage, P. B.; Fuangwasdi, S.; Lee, S. C.; Krakowiak, K. E.; Izatt, R. M. *J. Org. Chem.* **2001**, *66*, 4752–4758. (h) Dai, Z.; Xu, X.; Canary, J. W. *J. Chem. Soc., Chem. Commun.* **2002**, 1414–1415. (i) Jiang, P.; Chen, L.; Lin, J.; Liu, Q.; Ding, J.; Gao, X.; Guo, Z. *J. Chem. Soc., Chem. Commun.* **2002**, 1424–1425. (j) Gee, K. R.; Zhou, Z.-L.; Qian, W.-J.; Kennedy, R. *J. Am. Chem. Soc.* **2002**, *124*, 776–777. (k) Burdette, S. C.; Frederickson, C. J.; Bu, W.; Lippard, S. J. *J. Am. Chem. Soc.* **2003**, *125*, 1778–1787. (l) Hendrickson, K. M.; Geue, J. P.; Wyness, O.; Lincoln, S. F.; Ward, A. D. *J. Am. Chem. Soc.* **2003**, *125*, 3889–3895. (m) Sensi, S. L.; Ton-That, D.; Weiss, J. H.; Roth, A.; Gee, K. R. *Cell Calcium* **2003**, *34*, 281–284. (n) Taki, M.; Wolford, J. L.; O'Halloran, T. V. *J. Am. Chem. Soc.* **2004**, *126*, 712–713. (o) Henary, M. M.; Wu, Y.; Fahrni, C. J. *Chem. Eur. J.* **2004**, *10*, 3015–3025.

(26) Subat, M.; König, B. *Synthesis* **2001**, 1818–1825.

solvent was cooled and evaporated under reduced pressure, the remaining solids were crystallized from EtOH/H₂O to obtain **13**(NO₃)₂ as colorless prisms (0.85 g, 71% yield), mp 249–251 °C. IR (KBr): 3160, 3117, 2919, 1592, 1475, 1383, 1286, 1218, 1096, 1022, 979, 790, 593 cm⁻¹. ¹H NMR (D₂O): δ 2.64–2.67 (m, 2H), 2.82–2.93 (m, 6H), 3.01–3.11 (m, 4H), 3.35–3.48 (m, 4H), 7.65 (ddd, 1H, *J* = 7.8, 5.2, 1.8 Hz), 7.74 (d, 1H, *J* = 8.3 Hz), 8.24 (ddd, 1H, *J* = 8.3, 7.8, 1.8 Hz), 8.45 (m, 1H). ¹³C NMR (D₂O): δ 47.66, 47.69, 47.95, 54.47, 122.85, 127.95, 146.14, 150.35, 160.98. Anal. Calcd for C₁₃H₂₃N₇O₆-Zn: C, 35.59; H, 5.28; N, 22.35. Found: C, 35.28; H, 5.21; N, 22.27.

Zinc(II) 1-(2-Pyridyl)-1,4,7,10-tetraazacyclododecane-Phthalimide Complex, (ZnL6-PTI⁻) (22). ZnL6(NO₃)₂ (**13**(NO₃)₂) (98 mg, 0.22 mmol) and phthalimide potassium salt (42 mg, 0.22 mmol) were dissolved in an aqueous solution, and the pH of the mixture was adjusted to pH 7.0. After concentration of the whole under reduced pressure, the ZnL6-PTI⁻ complex (**22**) was obtained as colorless prisms (70 mg, 58% yield), mp >270 °C. IR (KBr): 3246, 3195, 2923, 1731, 1658, 1595, 1482, 1432, 1383, 1311, 1121, 990, 730 cm⁻¹. ¹H NMR (D₂O): δ 2.87–2.91 (m, 2H), 3.01–3.15 (m, 8H), 3.24–3.34 (m, 2H), 3.76–3.81 (m, 2H), 6.74 (dd, 1H, *J* = 7.4, 3.9 Hz), 6.96 (d, 1H, *J* = 8.5 Hz), 7.34 (dd, 1H, *J* = 8.5, 7.4 Hz), 7.55–7.56 (m, 2H), 7.86–7.69 (m, 2H), 7.94 (d, 1H, *J* = 3.9 Hz). ¹³C NMR (D₂O): δ 46.62, 47.93, 53.33, 124.91, 130.07, 130.74, 133.38, 136.32, 137.62, 149.83, 162.43, 184.04. Anal. Calcd for C₂₁H₂₇N₇O₅Zn: C, 48.24; H, 5.21; N, 18.75. Found: C, 47.91; H, 5.11; N, 18.99.

Crystallographic Study of 13(NO₃)₂ (ZnL6(NO₃)₂). A colorless prismatic crystal of **13**(NO₃)₂ (C₁₃H₂₃N₇O₆Zn, *M_r* = 438.75) having approximate dimensions of 0.20 mm × 0.20 mm × 0.15 mm was mounted in a loop. Intensity data were collected on a Rigaku RAXIS-RAPID imaging plate diffractometer with MoKα radiation. Cell constants and an orientation matrix for data collection corresponded to a primitive monoclinic cell with dimensions *a* = 20.0593(1) Å, *b* = 12.3531(3) Å, *c* = 19.9316(4) Å, β = 132.735(1)°, and *V* = 3627.6(1) Å³. For *Z* = 8 and *M_r* = 438.75, the calculated density (*D_{calcd}*) was 1.61 g·cm⁻³. Based on the systematic absence of *h*0*l* (*l* ≠ 2*n*), 0*k*0 (*k* ≠ 2*n*), the space group was uniquely determined to be *P*₂/1*c* (No. 14). The data were collected at -180 ± 1 °C to a maximum 2θ value of 60.1°. A total of 44 images, corresponding to 220.0° oscillation angles, were collected with two different goniometer settings. Data were processed by the PROCESS-AUTO program package. Of the 42 020 reflections collected, 10 416 were unique (*R_{int}* = 0.042); equivalent reflections were merged. The linear absorption coefficient for MoKα radiation, μ, is 14.0 cm⁻¹. A symmetry-related absorption correction using the ABSCOR program was applied which resulted in transmission factors ranging from 0.68 to 0.81. The structure was solved by direct methods (SHELXS86) and expanded by means of Fourier techniques (DIRDIF 94). The final cycle of full-matrix least-squares refinement (SHELXL-97) was based on 10 410 observed reflections (*I* > -3.00σ(*I*), 2θ < 60.06) and 487 variable parameters and converged (the largest parameter shift was 0.00 times its esd) with unweighted and weighted agreement factors of *R* [=Σ(*F_o*² - *F_c*²)/Σ*F_o*²] = 0.046 and *R_w* [=Σ(*w*(*F_o*² - *F_c*²)/Σ(*w*(*F_o*²))^{0.5})] = 0.047. The standard deviation of an observation of unit weight was 1.07. The maximum and minimum peaks on the final difference Fourier map corresponded to 0.77 and -0.62 e⁻·Å⁻³, respectively. All calculations were performed with the teXsan crystallographic software package from Molecular Structure Corp. (1985, 1999).

Crystallographic Study of ZnL6-PTI⁻ Complex (22). A colorless prismatic crystal of ZnL6-PTI⁻ complex (**22**) (C₂₁H₂₇N₇O₅Zn, *M_r* = 522.87) having approximate dimensions of 0.20 mm × 0.10 mm × 0.10 mm was mounted in a loop. Intensity data were collected on a Rigaku RAXIS-RAPID imaging plate diffractometer with MoKα radiation. Cell constants and an orientation matrix for data collection corresponded to a primitive monoclinic cell with dimensions *a* = 12.4268(3) Å, *b* = 11.8353(4) Å, *c* = 15.8009(5) Å, β = 102.830(2)°, and *V* = 2265.9(1) Å³. For *Z* = 4 and *M_r* = 522.87, the calculated

density (*D_{calcd}*) is 1.53 g·cm⁻³. Based on the systematic absence of *h*0*l* (*h* + *l* ≠ 2*n*), 0*k*0 (*k* ≠ 2*n*), the space group was uniquely determined to be *P*₂/1*c* (No. 14). The data were collected at -180 ± 1 °C to a maximum 2θ value of 60.0°. A total of 44 images, corresponding to 220.0° oscillation angles, were collected with two different goniometer settings. Data were processed by the PROCESS-AUTO program package. Of the 26 575 reflections collected, 6570 were unique (*R_{int}* = 0.023); equivalent reflections were merged. The linear absorption coefficient for MoKα radiation, μ, is 11.3 cm⁻¹. A symmetry-related absorption correction using the ABSCOR program was applied, resulting in transmission factors ranging from 0.80 to 0.89. The structure was solved by direct methods (SIR97) and expanded by means of Fourier techniques (DIRDIF 94). The final cycle of full-matrix least-squares refinement (SHELXL-97) was based on 6560 observed reflections (*I* > -3.00σ(*I*), 2θ < 60.02) and 307 variable parameters and converged (the largest parameter shift was 0.00 times its esd) with unweighted and weighted agreement factors of *R* [=Σ(*F_o*² - *F_c*²)/Σ*F_o*²] = 0.054, *R_w* [=Σ(*w*(*F_o*² - *F_c*²)/Σ(*w*(*F_o*²))^{0.5})] = 0.097. The standard deviation of an observation of unit weight was 1.04. The maximum and minimum peaks on the final difference Fourier map corresponded to 0.55 and -0.38 e⁻·Å⁻³, respectively. All calculations were performed with the teXsan crystallographic software package from Molecular Structure Corp. (1985, 1999).

UV Spectrophotometric and Fluorescence Titrations. UV spectra and fluorescence emission spectra were recorded on a Hitachi U-3500 spectrophotometer and a Hitachi F-4500 fluorescence spectrophotometer, respectively, at 25.0 ± 0.1 °C. For fluorescence titrations, a sample solution in a 1.0 mm quartz cuvette was excited at the isosbestic points determined by UV titrations. The obtained data of UV titrations (changes in ε values at a given wavelength) and fluorescence titrations (increases in fluorescence emission intensity at a given wavelength) were analyzed for apparent complexation constants, *K_{app}*, using the Bind Works program (Calorimetry Sciences Corp). Quantum yields were determined by comparison of the integrated corrected emission spectrum of standard *p*-terphenyl, which was excited at 265 nm in cyclohexane (quantum yield (Φ) is 0.87).²⁷ The fluorescence emission spectra of **L5** (**10**), **L6** (**11**), and their Zn²⁺ complexes were separated into the LE and TICT emissions by using the “Spectra Manager for Windows 95/98/NT (Curve Fitting)” program (JASCO International, Tokyo, Japan).

Potentiometric pH Titrations. Preparation of the test solutions and the method for calibrating the electrode system (Potentiometric Automatic Titrator AT-400 and Auto Piston Buret APB-410 (Kyoto Electronics Manufacturing, Co. Ltd.) with Orion Research Ross Combination pH Electrode 8102BN) were described earlier.^{9–17,22} All the test solutions (50 mL) were kept under an argon (>99.999% purity) atmosphere. The potentiometric pH titrations were performed with *I* = 0.10 (NaNO₃) at 25.0 ± 0.1 °C, and at least two independent titrations were performed (0.1 M aqueous NaOH was used as a base). Deprotonation constants of Zn²⁺-bound water, *K'₂* (= [HO⁻-bound species]/[H⁺]/[H₂O-bound species]), were determined by means of the “BEST” program.²⁸ All the sigma fit values defined in the program were smaller than 0.1. The *K_w* (= *a_H*⁺*a_{OH}*⁻), *K'_w* (= [H⁺][OH⁻]), and *f_H*⁺ values used at 25 °C are 10^{-14.00}, 10^{-13.79}, and 0.825. The corresponding mixed constants, *K₂* (= [HO⁻-bound species]_{aH}⁺/[H₂O-bound species]), were derived using [H⁺] = *a_H*⁺/*f_H*⁺. The species distribution values (%) against pH (= -log [H⁺] + 0.084) were obtained using the “SPE” program.²⁸

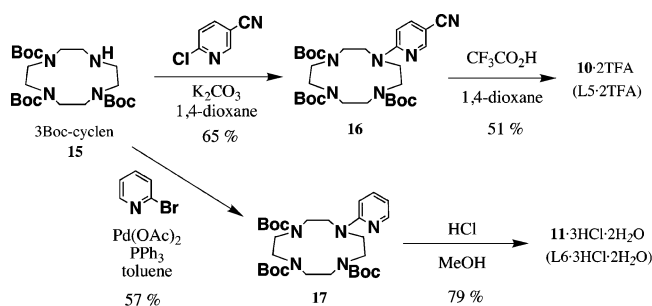
Results and Discussion

Synthesis of 10 (L5) and 11 (L6). New ligands **10** (L5) and **11** (L6) were synthesized as shown in Scheme 4. Reaction of

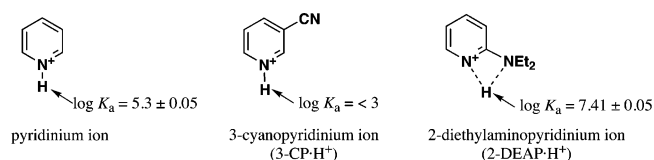
(27) Murov, S. L.; Carmichael, I.; Hug, G. L. *Handbook of Photochemistry*, 2nd ed.; Marcel Dekker: New York, 1993.

(28) Martell, A. E.; Motekaitis, R. J. *Determination and Use of Stability Constants*, 2nd ed.; VCH: New York, 1992.

Scheme 4

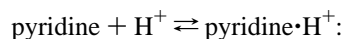


Scheme 5



2-chloro-5-cyanopyridine with 3Boc-cyclen **15**^{14b} gave **16**, and its Boc groups were removed with trifluoroacetic acid (TFA) to yield **10** as L5·2TFA. *N*-Arylation of **15** with 2-bromopyridine yielded **17**,²⁶ whose Boc groups were deprotected by aqueous HCl to give **11** as the 3HCl salt (L6·3HCl·2H₂O). The structure of L6·3HCl was confirmed by X-ray crystal structure analysis.²⁹

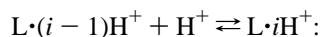
Protonation Constants of Reference Compounds, Pyridine, 3-Cyanopyridine (3-CP), and 2-Diethylaminopyridine (2-DEAP), Determined by Potentiometric pH and ¹H NMR Titrations. By potentiometric pH titrations, the protonation constants (defined by eq 1, where a_{H^+} is the activity of H⁺),



$$K_a = [\text{pyridine}\cdot\text{H}^+]/[\text{pyridine}]a_{\text{H}^+} \quad (1)$$

log K_a , of the reference pyridine derivatives, pyridine, 3-cyanopyridine (3-CP),³⁰ and 2-diethylaminopyridine (2-DEAP),³¹ were determined to be 5.3 ± 0.05 , <3 , and 7.41 ± 0.05 (Scheme 5), respectively.³² The ¹H NMR spectra (aromatic protons) of 2-DEAP (2 mM) in D₂O at various pD's showed significant change between pD 5.0 and pD 8.8, supporting the log K_a of 7.4 (Figure S2 in the Supporting Information). These data imply that the basicity of the pyridine moieties is strengthened by a dialkylamino moiety at the 2-position and weakened by a cyano group.

Protonation Constants of 10 (L5) and 11 (L6), Determined by Potentiometric pH, ¹H NMR, UV Spectrophotometric, and Fluorometric Titrations. The protonation constants, log K_{ai} ($i = 1-4$), of **10** (L5) and **11** (L6), defined by eq 2,



$$K_{ai} = [\text{L}\cdot i\text{H}^+]/[\text{L}\cdot(i-1)\text{H}^+]a_{\text{H}^+} \quad (2)$$

$$(\text{L} = \text{L5 or L6}, i = 1-4)$$

were examined by potentiometric pH titrations of a mixture of

(29) For the X-ray crystal structure of 11·3HCl·2H₂O (L6·3HCl·2H₂O), see Figure S1 in the Supporting Information. In a crystal, H₃L6 was found to take a planar conformation.

(30) The log K_a value of 3-cyanopyridine was reported to be 1.2 (Bellobono, I. R.; Monetti, M. A. *J. Chem. Soc., Perkin Trans. 2* **1973**, 790–793).

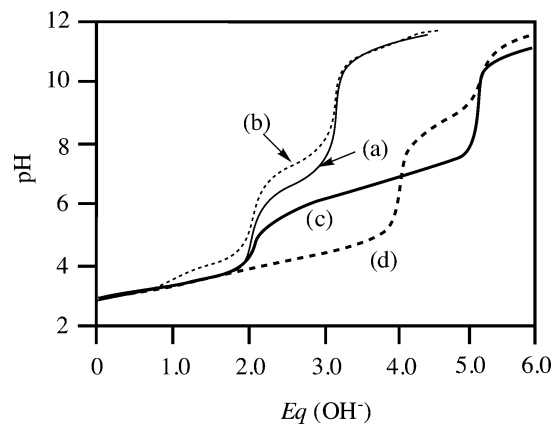


Figure 1. Typical potentiometric pH titration curves for (a) 1 mM L5·2TFA + 2 mM HNO₃, (b) 1 mM L6·3HCl + 1 mM HNO₃, (c) 1 mM L5·2TFA + 2 mM HNO₃ + 1 mM ZnSO₄, and (d) 1 mM L6·3HCl + 1 mM HNO₃ + 1 mM ZnSO₄ at 25 °C with $I = 0.1$ (NaNO₃). $Eq(\text{OH}^-)$ is the number of equivalents of base (NaOH) added.

1 mM of L5·2TFA + 2 mM HNO₃ and 1 mM L6·3HCl·2H₂O + 1 mM HNO₃ against 0.1 M NaOH with $I = 0.1$ (NaNO₃) at 25 °C. The titration data of L5 and L6 (Figure 1) were analyzed for the acid–base equilibrium in eq 2 by using the “BEST” program,²⁸ and log K_{ai} values for these ligands are summarized in Table 1. The log K_{a1} , log K_{a2} , and log K_{a4} values of L5 were assigned to protonation constants of three secondary amines in a cyclen ring by analogy with the log K_a values for [12]aneN₃ (L1)⁸ and 2,4-dinitrophenylcyclen **18** (L7) (Scheme 6),²² which were proven to be tridentate ligands for Zn²⁺ (Table 1). The log K_a values (<3) for a pyridinium proton of L5 were confirmed by the ¹H NMR titrations in D₂O at various pD's ([L5] = 2 mM), which showed a large shift of aromatic proton signals of L5 between pD ~2 and pD 3.7 (Figure S3 in the Supporting Information). The protonation behavior of L5 is summarized in Scheme 7.

From curve b in Figure 1, the log K_{ai} values ($i = 1-4$) for **11** (L6) were determined as listed in Scheme 7 and Table 1. The log K_{a3} value of 3.91 was assigned to the pyridinium ion by analogy with the log K_{a3} values for L5 and from the ¹H NMR spectral change (aromatic region) of L6 between pD ~2 and 5.9 (Figure S3 in the Supporting Information).

The log K_{ai} values of **10** (L5) and **11** (L6) were confirmed by UV and fluorometric titrations. A dashed curve (a) in Figure 2 shows a pH-dependent change of the molar absorption coefficients at 320 nm (ϵ_{320}) of 2-DEAP. From the decreasing sigmoidal curve, the log K_a value was calculated to be 7.5 ± 0.2 , which agreed with the log K_a of 7.41 obtained by potentiometric pH titrations. Curves b and c show pH-dependent changes of ϵ_{280} for L5 and ϵ_{310} for L6 and 25 °C, from which the log K_a values were calculated to be 6.6 ± 0.2 for L5, and 7.3 ± 0.2 and 3.8 ± 0.2 for L6, respectively.³³ These values show good agreement with the log K_a values for L5 (log $K_{a2} =$

(31) 2-DEAP was synthesized by a coupling reaction of diethylamine with 2-bromopyridine (3 equiv) in the presence of Pd(OAc)₂ (0.02 equiv), dicyclohexylphosphinobiphenyl (0.04 equiv), and NaOrBu (1.5 equiv) in toluene.

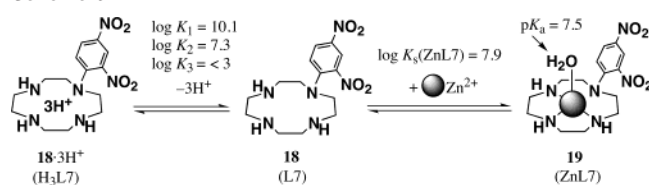
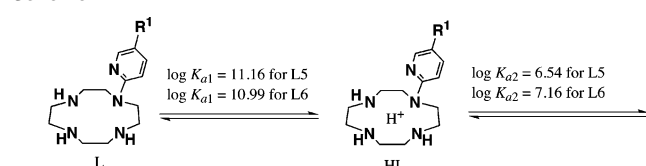
(32) The log K_a values of 2-aminopyridinium ion have been reported to be 6.71 (ref 30) and 6.94 (Forsythe, P.; Frampton, R.; Johnson, C. D.; Katritzky, A. Z. *J. Chem. Soc., Perkin Trans. 2* **1972**, 671–673), respectively, at 25 °C.

(33) For detailed pH-dependent change of UV spectra of L6 (0.2 mM) at 25 °C, see Figure S4 in the Supporting Information.

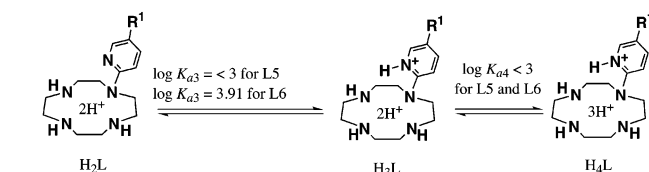
Table 1. Protonation Constants (K_a) and Complexation Constants of [12]janeN₃ (L1), Cyclen (L2), 2,4-Dinitrophenylcyclen **18** (L7), **10** (L5), and **11** (L6) at 25 °C with $I = 0.10$ (NaNO₃)^a

	[12]janeN ₃ (L1) ^b	cyclen (L2) ^c	18 (L7) ^d	10 (L5)	11 (L6)
log K_{a1}	12.6	11.0	10.1	11.16 ± 0.05 ^e	10.99 ± 0.05 ^e
log K_{a2}	7.6	9.9	7.33	6.54 ± 0.05 ^e	7.16 ± 0.05 ^e
log K_{a3}	2.4	<3	<3	<3 ^{e,f}	3.91 ± 0.05 ^{e,f}
log K_{a4}		<3		<3 ^e	<3 ^e
log $K_s(\text{ZnL})^a$	8.4 ^e	15.3 ^e	7.9 ^e	8.5 ± 0.1 ^e	11.3 ± 0.1 ^e
p <i>K</i> _a (ZnL) ^g	7.3	7.9	7.5	7.31 ± 0.05 ^e	8.37 ± 0.05 ^e
log $K_{\text{app}}(\text{ZnL})^i$ at pH 7.0	2.4	8.6	4.5	4.5 ± 0.1 ^e	6.4 ± 0.1 ^e
				4.2 ± 0.1 ^j	6.2 ± 0.1 ^k
				4.3 ± 0.2 ^l	6.1 ± 0.1 ^m
log $K_{\text{app}}(\text{ZnL})^n$ at pH 10.8	10.1	17.9	11.1	8.0 ± 0.1 ^e	11.1 ± 0.1 ^e
				7.5 ± 0.1 ^k	>8 ^k
				7.6 ± 0.2 ^m	>8 ^m

^a For the definition of $K_s(\text{ZnL})$, $K_{\text{app}}(\text{ZnL})$, and p*K*_a(ZnL), see the text. ^b From ref 9a at 25 °C with $I = 0.1$ (NaNO₃). ^c From ref 15c at 25 °C with $I = 0.1$ (NaNO₃). ^d From ref 22 at 25 °C with $I = 0.1$ (NaNO₃). ^e Determined by potentiometric pH titrations. ^f log K_a values for pyridinium protons. ^g p*K*_a values for Zn²⁺-bound water in the Zn²⁺ complexes. ^h Determined by fluorometric titrations at [L] = 0.1 mM. ⁱ Apparent complexation constants at pH 7.0 with $I = 0.1$ (NaNO₃). ^j Determined by UV titrations at [L] = 25 μM. ^k Determined by UV titrations at [L] = 50 μM. ^l Determined by fluorometric titrations at [L] = 0.1 mM. ^m Determined by fluorometric titrations at [L] = 50 μM. ⁿ Apparent complexation constants at pH 10.8 with $I = 0.1$ (NaNO₃).

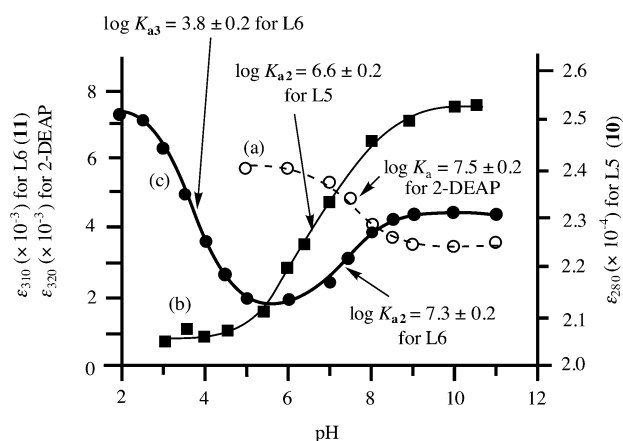
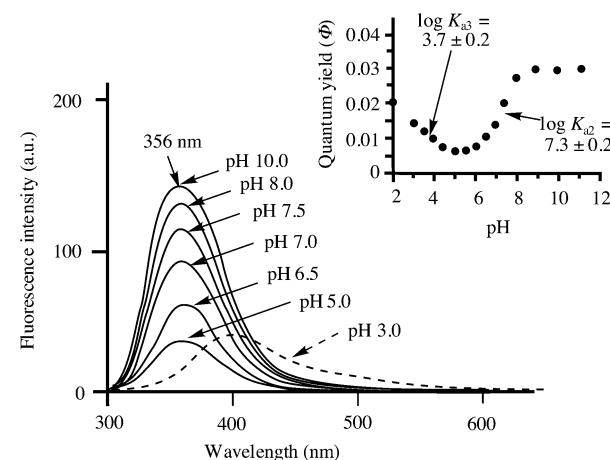
Scheme 6**Scheme 7**

L = L5 (R¹ = CN) or L6 (R¹ = H)



6.54) and L6 (log $K_{a2} = 7.16$ and log $K_{a3} = 3.91$) obtained by potentiometric pH titrations.

Figure 3 depicts fluorescence emission spectra of L6 (0.2 mM) at pH 3.0, 5.0, 6.5, 7.0, 7.5, 8.0, and 10.0, showing that the emission increases as the pH rises (excitation at 265 nm, which is an isosbestic point determined by UV titrations). The quantum yields (Φ) of L6 in the pH range pH 2.0–11.0 are plotted in the inset of Figure 3, which looks similar to the bold curve (c) in Figure 2. The log K_a values of 7.3 ± 0.2 (log K_{a2}) and 3.7 ± 0.2 (log K_{a3}) estimated from Figure 3 agree well with the log K_{a2} and log K_{a3} values of L6 obtained by potentiometric pH titrations. These results also indicate that the log K_a values of L6 at ground states (by potentiometric pH and UV spectroscopic titrations) are almost identical with those at excited states (by fluorescence titrations). The lower log K_{a3} value (3.91) for the pyridine moiety of L6 than that (7.41) of 2-DEAP (Scheme 5) suggests that the H₃L6 form is destabilized by electrostatic repulsion between a pyridinium cation and a diprotonated cyclen ring (see Scheme 7). A dashed curve in Figure 3 shows an emission spectrum of L6 at pH 3.0, which has an emission maximum at ~400 nm, suggesting the partial

**Figure 2.** pH-dependent change of molar absorption coefficients (ϵ) in UV spectra of (a) 2-DEAP, (b) L5, and (c) L6 at 25 °C with $I = 0.1$ (NaNO₃). [2-DEAP] = [L5] = [L6] = 0.2 mM.**Figure 3.** pH-dependent change in fluorescence emission of L6 (0.2 mM) at pH 3.0 (a dashed curve), 5.0, 6.5, 7.0, 7.5, 8.0, and 10.0 (plain curves) in aqueous solution at 25 °C (excitation at 265 nm) with $I = 0.1$ (NaNO₃) (a.u. is arbitrary unit). The inset implies a pH-dependent change of quantum yields (Φ) of L6.

contribution of intramolecular exciplex formation^{6e} due to protonation of the pyridine nitrogen.

UV Spectrophotometric and Fluorometric Titrations of **10 (L5) and **11** (L6) with Zn²⁺.** UV and fluorescence titrations of **10** (L5) and **11** (L6) with Zn²⁺ were performed at pH 7.0

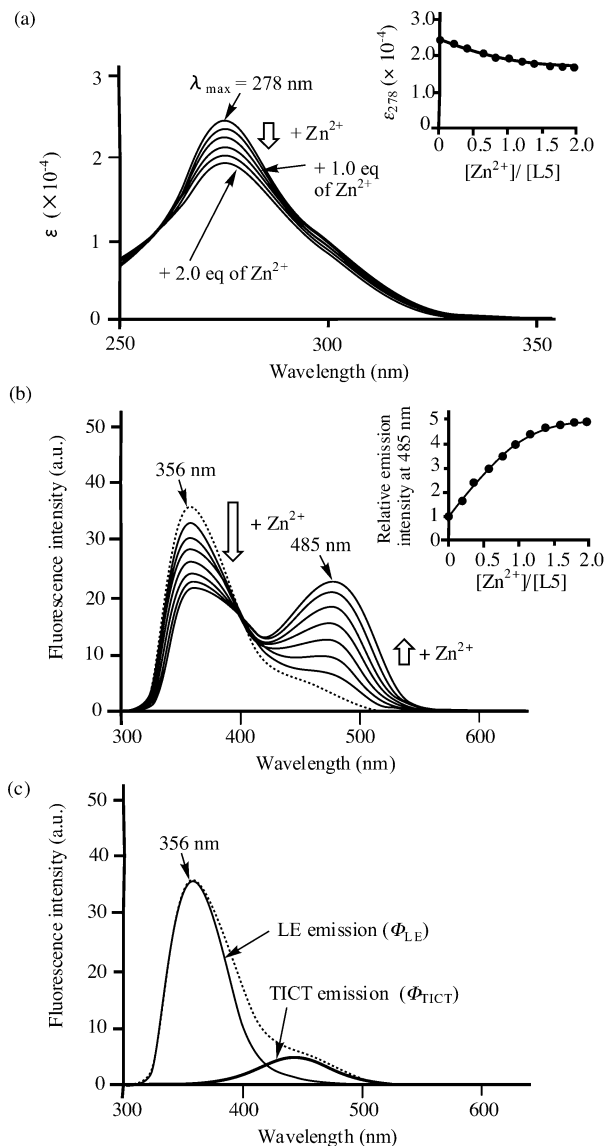


Figure 4. (a) UV absorption spectral change of L5 (25 μM) upon addition of Zn²⁺ at pH 7.0 (10 mM HEPES with *I* = 0.1 (NaNO₃)) and 25 °C. The inset is the titration curve (decreasing ε₂₇₈) of L5 with Zn²⁺ at pH 7.0 (10 mM HEPES with *I* = 0.1 (NaNO₃)) and 25 °C. (b) Change in fluorescence emission of L5 (0.1 mM) upon addition of Zn²⁺ at pH 7.0 (10 mM HEPES with *I* = 0.1 (NaNO₃)) and 25 °C (excitation at 260 nm). The inset shows an increase of relative emission intensity (*I*/*I*₀) of L5 at 485 nm upon addition of Zn²⁺ at pH 7.0 (10 mM HEPES with *I* = 0.1 (NaNO₃)) and 25 °C, where *I*₀ = emission intensity of L5 at 485 nm in the absence of Zn²⁺. (c) The LE and TICT emissions are separated using the fluorescence emission spectrum (a dashed curve in panel b) of L5 (0.1 mM) at pH 7.0 (10 mM HEPES with *I* = 0.1 (NaNO₃)) and 25 °C.

(10 mM HEPES with *I* = 0.1 (NaNO₃)) and 25 °C. As shown in Figure 4a, metal-free L5 (25 μM) has an absorption maximum at 278 nm (ε₂₇₈ = 2.5 × 10⁴), which decreased upon addition of Zn²⁺, as shown in the inset of Figure 4a.

The dashed curve in Figure 4b shows the emission spectrum of metal-free L5 (0.1 mM), having an emission maximum at 356 nm (excitation at 260 nm) which is assignable to the emission from locally excited (LE) states. An addition of Zn²⁺ caused a gradual decrease in LE emissions at 356 nm and an increase of emissions at 485 nm. From the titration curves shown in the insets of Figure 4a,b, the apparent complexation constants defined by eqs 3 and 4, log *K*_{app}(ZnL5), were calculated to be

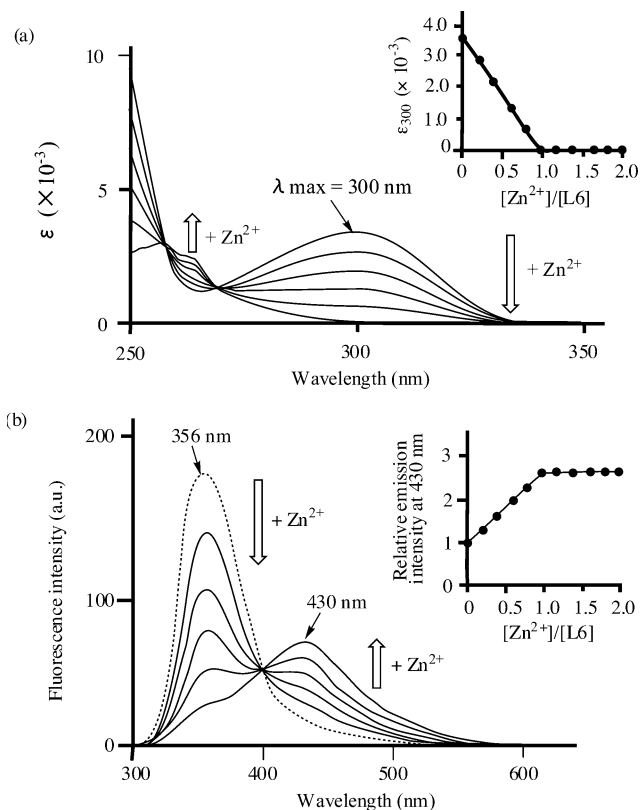


Figure 5. (a) UV absorption spectral change of L6 (0.2 mM) upon addition of ZnSO₄ at pH 7.0 (10 mM HEPES with *I* = 0.1 (NaNO₃)) and 25 °C. The inset is the titration curve (decreasing ε₃₀₀) of L6 with Zn²⁺ at pH 7.0 (10 mM HEPES with *I* = 0.1 (NaNO₃)) and 25 °C. (b) Change in fluorescence emission of L6 (0.2 mM) upon addition of ZnSO₄ at pH 7.0 (10 mM HEPES with *I* = 0.1 (NaNO₃)) and 25 °C (excitation at 260 nm). The inset shows an increase of relative emission intensity (*I*/*I*₀) of L6 at 430 nm upon addition of ZnSO₄ at pH 7.0 (10 mM HEPES with *I* = 0.1 (NaNO₃)) and 25 °C, where *I*₀ = emission intensity of L6 at 430 nm in the absence of Zn²⁺.

4.2 ± 0.2–4.3 ± 0.2, as listed in Table 1 (ZnL(H₂O) and ZnL(HO⁻) in eq 3 are a Zn²⁺-bound water form and a Zn²⁺-bound hydroxide form, respectively).³⁴

$$K_{\text{app}}(\text{ZnL}) = \frac{[\text{ZnL}(\text{H}_2\text{O}) + \text{ZnL}(\text{HO}^-)]}{[\text{L}]_{\text{free}}[\text{Zn}^{2+}]_{\text{free}}} \quad (\text{at designated pH}) \quad (\text{M}^{-1}) \quad (3)$$

$$[\text{L}]_{\text{free}} = [\text{L} \cdot 4\text{H}^+]_{\text{free}} + [\text{L} \cdot 3\text{H}^+]_{\text{free}} + [\text{L} \cdot 2\text{H}^+]_{\text{free}} + [\text{L} \cdot \text{H}^+]_{\text{free}} + [\text{L}]_{\text{free}} \quad (\text{L} = \text{L5 or L6}) \quad (4)$$

The UV and emission spectral changes of L6 (0.2 mM) upon addition of Zn²⁺ at pH 7.0 (10 mM HEPES with *I* = 0.1 (NaNO₃)) and 25 °C show a remarkable contrast to those for L5 (Figure 5). The UV absorption spectra (ε₃₀₀ = 4.0 × 10³ M⁻¹·cm⁻¹ in the absence of Zn²⁺) changed sharply with isosbestic points at 258 and 270 nm, as shown in Figure 5a. The emission spectral change of L6 (0.2 mM) upon addition of Zn²⁺ (Figure 5b) exhibits a linear decrease of emissions at 356 nm (excitation at 270 nm) and a linear increase of emissions at 430 nm (plotted in the inset of Figure 5b), strongly indicating 1:1 complexation.^{35–37} The log *K*_{app}(ZnL6) values at pH 7.0

(34) The quantum yields (Φ) of L5 (25 μM) at pH 7.0 (10 mM HEPES with *I* = 0.1 (NaNO₃)) and 25 °C in the absence and in the presence of 2 equiv of Zn²⁺ are 0.004 and 0.003, respectively.

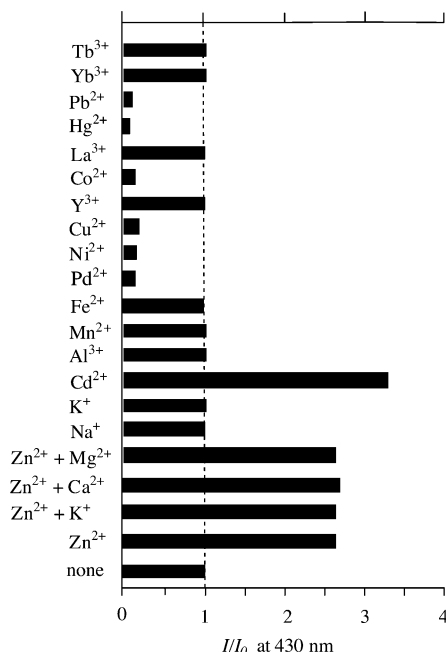


Figure 6. Fluorescence response of L6 (0.2 mM) against 1 equiv of various metal cations at pH 7.0 (10 mM HEPES with $I = 0.1$ (NaNO₃)) and 25 °C. I_0 and I are emission intensities of L6 at 430 nm in the absence and in the presence of metal ions, respectively. Excitation wavelengths were 257 nm for Cu²⁺, 268 nm for Ni²⁺, 282 nm for Pb²⁺, 291 nm for Hg²⁺, and 270 nm for Zn²⁺, Cd²⁺, Co²⁺, and other metals, which are isosbestic points determined by UV titrations.

were estimated to be 6.1 ± 0.1 – 6.2 ± 0.1 by UV and fluorometric titrations at [L6] = 50 μM.

The ¹H NMR spectra of 5 mM L5 and 5 mM L6 in the presence of 2.5 mM Zn²⁺ (0.5 equiv) in D₂O at pH 7.0 and 25 °C exhibited two independent sets of peaks for metal-free L5 or L6 and those for ZnL5 or ZnL6 (data not shown). In addition, aromatic signals of ZnL5 and ZnL6 appeared with considerable downfield shifts in comparison with those of L5 and L6 ($\Delta\delta = +0.2$ – 0.5 for ZnL5 and $+0.3$ – 0.7 for ZnL6). These facts indicate that ZnL5 and ZnL6 are kinetically stable on the NMR time scale and that pyridyl nitrogens coordinate to Zn²⁺.³⁸

Fluorescence Response of L6 to Metal Ions in Aqueous Solution. The fluorescence changes of L6 (0.2 mM) with other metal ions, such as Cd²⁺, Cu²⁺, Co²⁺, Ni²⁺, Fe²⁺, Pb²⁺, Al³⁺, Y³⁺, Li⁺, Na⁺, K⁺, Ca²⁺, and Mg²⁺, at pH 7.0 (10 mM HEPES with $I = 0.1$ (NaNO₃)) and 25 °C are summarized in Figure 6. Among these metals, only Zn²⁺ and Cd²⁺ induced TICT,^{39–41}

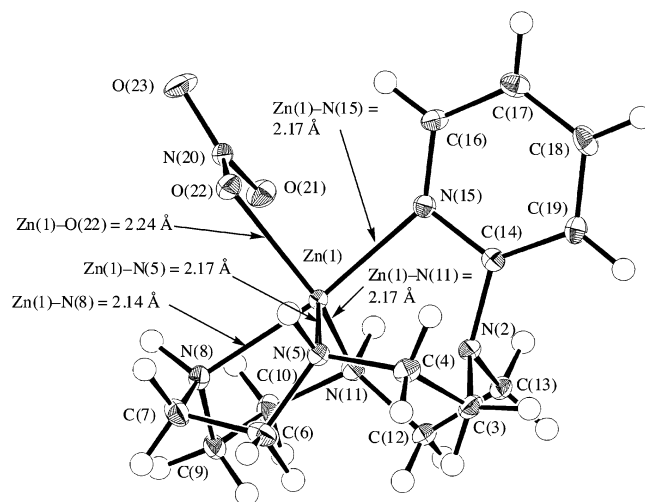


Figure 7. ORTEP drawing (50% probability ellipsoids) of the ZnL6-(NO₃)₂ complex (**13**(NO₃)₂). Selected bond distances (Å): Zn(1)–N(5) 2.166(1), Zn(1)–N(8) 2.140(1), Zn(1)–N(11) 2.168(1), Zn(1)–N(15) 2.168(1), Zn(1)–O(22) 2.245(1), N(2)–C(14) 1.434(2), C(14)–N(15) 1.340(2), N(15)–C(16) 1.343(2), C(16)–C(17) 1.380(2), C(17)–C(18) 1.382(2), C(18)–C(19) 1.382(2). Selected dihedral angles (deg): C(3)–N(2)–C(14)–N(15) 114.4, C(3)–N(2)–C(14)–C(19) –63.6, C(13)–N(2)–C(14)–N(15) –103.0, C(13)–N(2)–C(14)–C(19) 79.0, Zn(1)–N(15)–C(14)–N(2) 5.6.

and Cu²⁺ and Hg²⁺ quenched the emission of L6.^{42,43} TICT emissions of ZnL6 were not perturbed by Na⁺, K⁺, Mg²⁺, and Ca²⁺. Other metal ions did induce negligible changes in the emission spectra of L6.

X-ray Crystal Structure of the ZnL6 Complex (13). We have isolated fine colorless crystals from a mixture of L6 and Zn(NO₃)₂ in an aqueous solution at pH 7.0. Elemental analysis suggested the formula ZnL6(NO₃)₂. X-ray crystal structure analysis disclosed intramolecular coordination of N(15) of the pyridine group of L6 to Zn²⁺ as well as the three nitrogens (N(5), N(8), and N(11)) of a cyclen ring (Figure 7). The Zn²⁺–N(15) coordination bond length is 2.17 Å, which is almost the same length as those of the three Zn²⁺–N(cyclen) bonds (2.14–2.17 Å). It was also found that the Zn²⁺–N(2) coordination bond is somehow weak (Zn²⁺–N(2) bond length is 2.42 Å) and that Zn²⁺ has a trigonal bipyramidal geometry with the N(5), N(8), N(11), N(15), and NO₃ anion, which is similar to that of the Zn²⁺–dansylethylamide cyclen complex **7**.^{19a} The dihedral angles for C(3)–N(2)–C(14)–N(15) of 103.0° and for C(13)–N(2)–C(14)–N(15) of 114.4° clearly indicate a twisted conformation of the pyridine face with respect to the dialkylamino face comprising C(3)–N(2)–C(13). An external ligand NO₃[–] (Zn²⁺–O(22) = 2.24 Å) is considered to be replaced by an H₂O molecule.^{14b}

(35) Change in excitation spectra (emission at 430 nm) of L6 (0.2 mM) upon addition of Zn²⁺ at pH 7.0 (10 mM HEPES with $I = 0.1$ (NaNO₃)) and 25 °C is presented in Figure S5 in the Supporting Information.

(36) For comparison, the change of UV and emission spectra (excitation at 254 nm) of 2-DEAP (0.1 mM) upon addition of Zn²⁺ in CH₃CN at 25 °C is shown in Figure S6 in the Supporting Information. Emission of 2-DEAP (0.1 mM) at 365 nm was quantitatively quenched by Zn²⁺.

(37) The quantum yields (Φ) of L6 and ZnL6 at pH 7.0 (10 mM HEPES with $I = 0.1$ (NaNO₃)) are 0.013 and 0.010 (at [L6] or [ZnL6] = 0.2 mM, where ZnL6 is quantitatively formed), respectively.

(38) The stability of ZnL6 was further confirmed by fluorometric titrations in the presence of [12]aneN₃ (L1). At pH 7.0, an addition of 1–10 equiv of L1 had a negligible effect on the emission spectra of ZnL6, supporting that $\log K_{\text{app}}(\text{ZnL6})$ is much larger than $\log K_{\text{app}}(\text{ZnL1})$ of 2.4 at pH 7.0 (Table 1). In contrast, at pH 10.8, the emission intensity of ZnL6 at 351 nm was reduced by ca. 30% upon addition of 1 equiv of L1, suggesting that $\log K_{\text{app}}(\text{ZnL6})$ is close to the $\log K_{\text{app}}(\text{ZnL1})$ of 10.1. These facts imply that L6 behaves mainly as a tetradentate ligand to Zn²⁺ (through three NH's in cyclen and one pyridyl N) at pH 7.0 and as a tridentate ligand (through only three NH's in cyclen) at pH 10.8 (see the following sections).

(39) The quantum yields (Φ) of L6 (0.2 mM) changed from 0.013 to 0.010 upon addition of 1 equiv of Cd²⁺. The change in UV and emission spectra (excitation at 270 nm) of L6 (0.2 mM) upon addition of Cd²⁺ is presented in Figure S7 in the Supporting Information. The $\log K_{\text{app}}(\text{CdL6})$ and $\log K_{\text{app}}(\text{CuL6})$ at pH 7.0 and 25 °C were estimated to be >8 .

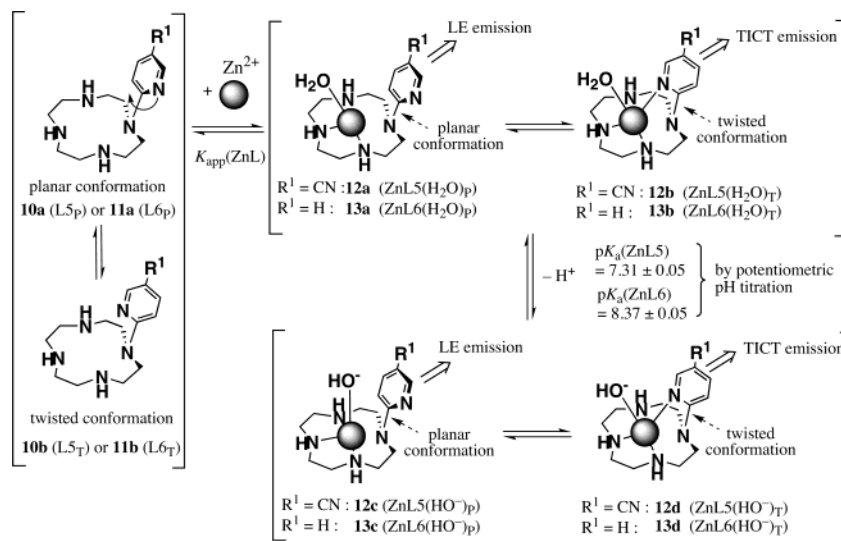
(40) The change in emission spectra of L5 (0.1 mM) upon complexation with Cd²⁺ at pH 7.0 (10 mM HEPES with $I = 0.1$ (NaNO₃)) is shown in Figure S8 in the Supporting Information (excitation at 250 nm). The $\log K_{\text{app}}(\text{CdL5})$ was 5.0 ± 0.2 .

(41) For Cd²⁺ sensors, see: Prodi, L.; Montalti, M.; Zaccheroni, N.; Savage, P. B.; Bradshaw, J. S.; Izatt, R. M. *Tetrahedron Lett.* **2001**, *42*, 2941–2944.

(42) For the emission spectral change of L6 (0.2 mM) upon addition of Cu²⁺ (excitation at 254 nm), see Figure S9 in the Supporting Information.

(43) For Cu²⁺ sensors, see: (a) Krämer, R. *Angew. Chem., Int. Ed.* **1998**, *37*, 772–773. (b) Prodi, L.; Montalti, M.; Zaccheroni, N.; Savage, P. B.; Bradshaw, J. S.; Izatt, R. M. *Tetrahedron Lett.* **2001**, *42*, 2941–2944. (c) Zheng, Y.; Gattás-Asfura, K. M.; Konka, V.; Leblanc, R. M. *J. Chem. Soc., Chem. Commun.* **2002**, 2350–2351.

Scheme 8



Hypothesis for Zn^{2+} Coordination Behaviors of L5 and L6. We have assumed two conformers, **10a** (L5_P) and **10b** (L5_T), for a metal-free L5, as depicted in Scheme 8 (subscripts P and T are abbreviations for the planar and twisted conformers, respectively). Emissions at shorter wavelengths (at 356 nm) of the metal-free L5 are considered to originate from L5_P, and emissions at ~450 nm are due to L5_T. The emission spectrum of L5 at pH 7.0 and 25 °C in Figure 4b (a dashed curve) was broken down into LE (a plane curve) and TICT (a bold curve) emissions^{6b,e} as shown in Figure 4c, and the LE:TICT ratio (Φ_{LE}/Φ_{TICT} : Φ_{TICT}/Φ_{total}) was calculated to be 82:18 (Φ_{LE} , Φ_{TICT} , and Φ_{total} are the quantum yields of LE and TICT and the total emissions of L5).

The Zn^{2+} complexation of L5 yields two forms of **12**: one is a Zn^{2+} -bound H₂O form, ZnL5(H₂O), and the other is its deprotonated form, ZnL5(HO⁻). For each form, we assume equilibria between planar conformers, **12a** (ZnL5(H₂O)_P) and **12c** (ZnL5(HO⁻)_P), in which a nitrogen in the pyridine rings hardly coordinates to Zn^{2+} , and twisted conformers, **12b** (ZnL5(H₂O)_T) and **12d** (ZnL5(HO⁻)_T), where a nitrogen in the pyridine rings coordinates to Zn^{2+} , resulting in emissions at longer wavelengths (Scheme 8). We consider that the LE:TICT (Φ_{LE}/Φ_{total} : Φ_{TICT}/Φ_{total}) ratio corresponds to the ratio of planar conformers and twisted conformers of L5 and ZnL5, that is, [(**10a** + **12a** + **12c**):(**10b** + **12b** + **12d**)]. Figure 8a shows that the TICT emissions gradually increase to 62% upon addition of Zn^{2+} (0–2 equiv).

Figure 8b displays that the LE:TICT ratio of 65:35 for a metal-free L6 (0.2 mM) linearly changed upon addition of Zn^{2+} and was almost saturated in the presence of an equimolar amount of Zn^{2+} ([(**13a** + **13c**):(**13b** + **13d**)] = 2:98),⁴⁴ indicating that TICT is efficiently controlled by the Zn^{2+} -N(pyridine) coordination in ZnL6.

Study of the Zn^{2+} Complexation Properties of L5 (10) and L6 (11) by Potentiometric pH Titrations. By analysis of the potentiometric pH titration curve for 1 mM L5 (curve c in Figure 1) in the presence of an equimolar amount of ZnSO₄ at 25 °C with $I = 0.1$ (NaNO₃), the 1:1 complexation constant of L5

with Zn^{2+} defined by eqs 5 and 7, $\log K_S(ZnL5)$, was determined to be 8.5 ± 0.1 (Table 1).⁴⁵ This value is similar to the $\log K_S(ZnL)$ values for **4** (8.4)⁹ and **19** (7.9)¹⁰ (Scheme 6), suggesting weak coordination of a 5-cyanopyridine moiety of L5 with Zn^{2+} . The deprotonation constant for the Zn^{2+} -bound water in ZnL5, defined by eq 6, $K_a(ZnL5)$, is 7.31 ± 0.05 , which is close to those for **4** (7.3)⁹ and **19** (7.5).¹⁰ The distribution diagram for a mixture of 1 mM L5 and 1 mM Zn^{2+} is shown in Figure 9a, in which the ZnL5(H₂O) is formed in about 50–60% yield at pH 6.0–7.1. The apparent complexation constant for ZnL5, defined by eqs 3, 4, 7, and 8, $\log K_{app}(ZnL5)$, at 25

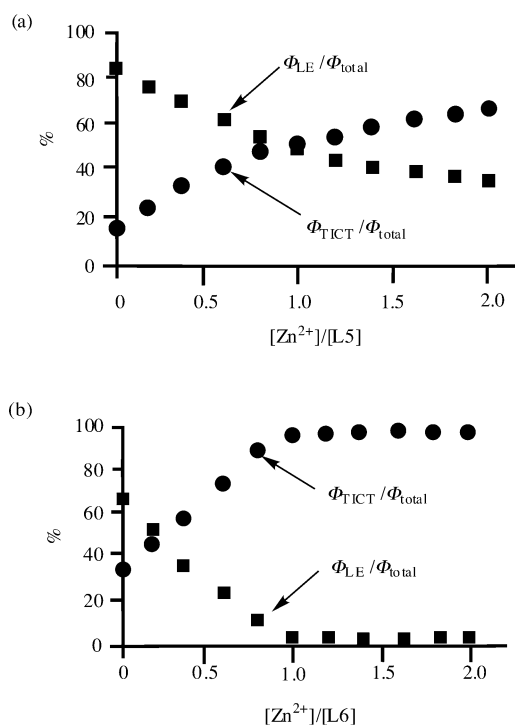


Figure 8. (a) Change in LE:TICT ratio (Φ_{LE}/Φ_{total} : Φ_{TICT}/Φ_{total}) for L5 (25 μ M) upon addition of ZnSO₄ at pH 7.0 (10 mM HEPES with $I = 0.1$ (NaNO₃)) and 25 °C (Φ_{LE}/Φ_{total} , solid squares; Φ_{TICT}/Φ_{total} , solid circles). (b) Change in LE:TICT ratio (Φ_{LE}/Φ_{total} : Φ_{TICT}/Φ_{total}) for L6 (0.2 mM) upon addition of Zn^{2+} at pH 7.0 (10 mM HEPES with $I = 0.1$ (NaNO₃)) and 25 °C.

(44) From the titration curve shown in the inset of Figure 5, the concentration of the metal-free L6 is considered to be negligible at $[L6]_{total} = [Zn^{2+}]_{total} = 0.2$ mM.

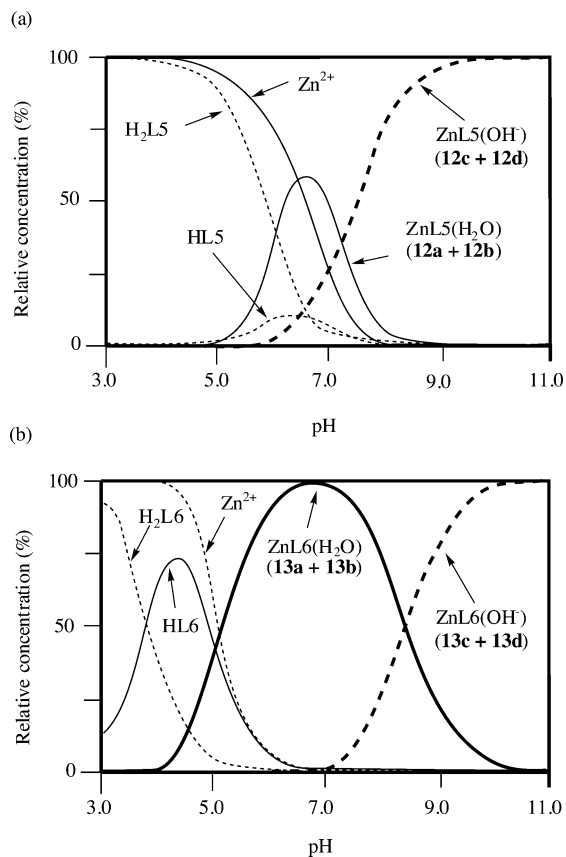
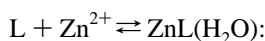


Figure 9. Distribution diagrams for (a) a mixture of 1.0 mM L5 + 1.0 mM Zn²⁺ and (b) a mixture of 1.0 mM L6 + 1.0 mM Zn²⁺ at 25 °C with $I = 0.1$ (NaNO₃).

°C and pH 7.0 with $I = 0.1$ (NaNO₃) was calculated to be 4.5 ± 0.1 .



$$K_s(ZnL) = [ZnL(H_2O)]/[L][Zn^{2+}] \quad (M^{-1}) \quad (5)$$



$$K_a(ZnL) = [ZnL(HO^-)]a_{H^+}/[ZnL(H_2O)] \quad (6)$$

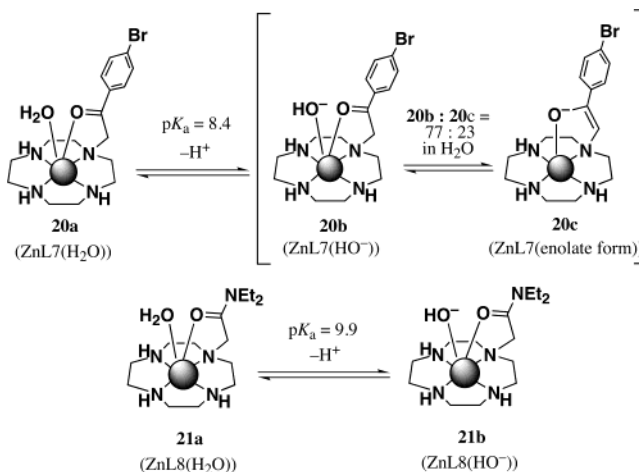
$$[ZnL(H_2O)] = [12a] + [12b] \text{ for ZnL5 or } [13a] + [13b] \text{ for ZnL6} \quad (7)$$

$$[ZnL(HO^-)] = [12c] + [12d] \text{ for ZnL5 or } [13c] + [13d] \text{ for ZnL6} \quad (8)$$

Similarly, the log $K_s(ZnL6)$ was determined to be 11.1 ± 0.1 (from curve d in Figure 1), which is larger than those for **4** (8.4),⁹ **12** (8.5), and **19** (7.9),²² and smaller than that for Zn²⁺-cyclen **5** (15.3), supporting a Zn²⁺-N(pyridine) coordination in ZnL6. The distribution diagram at $[Zn^{2+}] = [L6] = 1$ mM in Figure 9b indicates that ZnL6 is formed almost quantitatively at pH 7.0. The log $K_{app}(ZnL6)$ at pH 7.0 and 25 °C is $6.4 \pm$

(45) It should be noted that the $K_s(ZnL)$ values for ZnL5 or ZnL6 in eqs 5–8 are defined as averaged complexation constants for **12a** (or **13a**) (ligands are tetradentate) and **12b** (or **13b**) (ligands are tridentate), which are indistinguishable by pH titrations. The apparent complexation constants at the designated pH, $K_{app}(ZnL)$, which were calculated from $K_s(ZnL)$ values obtained by potentiometric pH titrations, agree well with the $K_{app}(ZnL)$ obtained by UV spectroscopic and fluorescence titrations.

Scheme 9



0.1, which is identical to the log $K_{app}(ZnL6)$ of 6.1–6.2 obtained by UV and fluorescence titrations (Table 1).

The pK_a value (defined by eqs 6–8) of Zn²⁺-bound water in ZnL6 is 8.37 ± 0.05 , which is larger than the $pK_a(ZnL)$ values for **4** (7.3),⁹ **12** (7.31), and **19** (7.5).²² Previously, we had found that Zn²⁺ complexes **20** (ZnL7)⁴⁶ and **21** (ZnL8),⁴⁷ which have additional Zn²⁺-chelating side chains, possess larger pK_a values than those for **5** ($pK_a = 8.4$ for $20a \rightleftharpoons 20b + 20c$ ⁴⁶ and $pK_a = 9.9$ for $21a \rightleftharpoons 21b$ ⁴⁷) (Scheme 9). These facts have also proven that the pyridine group of L6 chelates to Zn²⁺ in ZnL6.

pH-Dependent Change of Fluorescence Emission of **13** (ZnL6) and Sensing of Succinimide by **13**.

Figure 10 shows

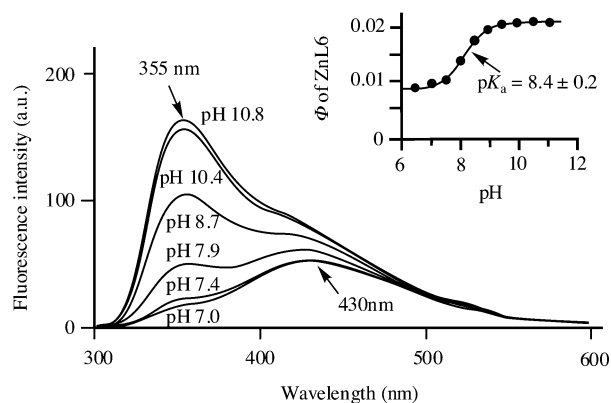


Figure 10. pH-dependent change of emission spectra of ZnL6 (0.2 mM) in 10 mM Good's buffer with $I = 0.1$ (NaNO₃) at 25 °C (excitation at 270 nm). The inset shows a change of quantum yields of ZnL6, giving the pK_a values for Zn²⁺-bound water of 8.4 ± 0.2 .

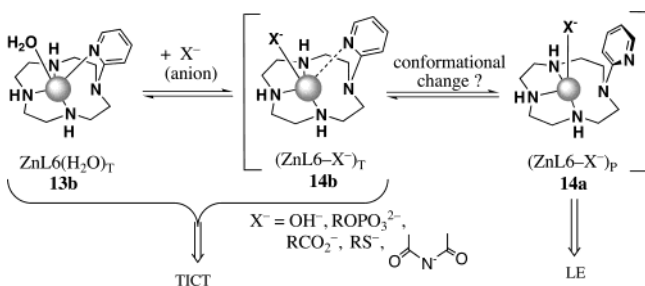
the emission spectra of ZnL6 (0.2 mM) in the pH range 7.0–10.8 at 25 °C with $I = 0.1$ (NaNO₃) (excitation at 270 nm). From the pH– Φ profile in the inset, the $pK_a(ZnL6)$ value was determined to be 8.4 ± 0.2 at 25 °C, which is very close to the $pK_a(ZnL6)$ value determined by potentiometric pH titration. The LE:TICT ratio of ZnL6 at pH 10.8 was 35:65, indicating that TICT was released in an alkaline solution.

We thus hypothesized that the microenvironment around Zn²⁺ in ZnL6 may affect the conformation of the pyridine ring, as depicted in Scheme 10. Namely, an electron donation from OH⁻

(46) Kimura, E.; Gotoh, T.; Aoki, S.; Shiro, M. *Inorg. Chem.* **2002**, *41*, 3239–3248.

(47) Kimura, E.; Gotoh, T.; Koike, T.; Shiro, M. *J. Am. Chem. Soc.* **1999**, *121*, 1267–1274.

Scheme 10



or other anions (X^-) and/or their steric hindrance may weaken the Zn^{2+} -N(pyridine) coordination bond and induce a conformational change from the twisted form **14b** ($[\text{ZnL6-X}^-]_T$) to the planar form **14a** ($[\text{ZnL6-X}^-]_P$), allowing emission shifts from TICT to LE.⁴⁸

This hypothesis prompted us to examine the fluorescence response of ZnL6 to anions at neutral pH, because it is known that the Zn^{2+} -cyclen complexes recognize imide anions,^{15,16} carboxylates,^{10,13} phosphate monoester dianions,¹⁴ and thiolates^{11,17} in aqueous solution. Figure 11a shows the emission spectral change of ZnL6 (0.2 mM, where ZnL6 is quantitatively formed) upon addition of succinimide (SI, see Scheme 11 for its structure) at pH 7.0 (50 mM HEPES with $I = 0.1$ (NaNO_3)) and 25 °C. As plotted in Figure 11b, the LE emission at 351 nm was enhanced and the TICT emission at 430 nm from TICT was suppressed by the addition of SI. From the bold curve (a) in Figure 12, plotting the relative emission intensity at 355 nm at increasing concentrations of SI, the apparent complexation constant for the ZnL6-SI^- complex, defined by eqs 9–11, $\log K_{\text{app}}(\text{ZnL6-X}^-)$, was calculated to be 2.8 ± 0.1 (Table 2).

$\text{ZnL6} + \text{guest} (\text{X}) \rightleftharpoons \text{ZnL6-X}^-$ complex:

$$K_{\text{app}}(\text{ZnL6-X}^-) = \frac{[\text{ZnL6-X}^- \text{ complex}]}{[\text{X}]_{\text{free}}[\text{ZnL6}]_{\text{free}}} \quad (9)$$

$$[\text{ZnL6}]_{\text{free}} = \frac{[\text{ZnL6}(\text{H}_2\text{O})_7(\mathbf{13a} + \mathbf{13b})]_{\text{free}} + [\text{ZnL6}(\text{HO}^-)(\mathbf{13c} + \mathbf{13d})]_{\text{free}}}{[\text{ZnL6}(\text{H}_2\text{O})_7(\mathbf{13a} + \mathbf{13b})]_{\text{free}} + [\text{ZnL6}(\text{HO}^-)(\mathbf{13c} + \mathbf{13d})]_{\text{free}}} \quad (10)$$

$$[\text{X}]_{\text{free}} = [\text{X}]_{\text{free}} + [\text{X}^-]_{\text{free}} + \dots + [\text{X}^{n-}]_{\text{free}} \quad (11)$$

The interactions of ZnL6 (0.2 mM) with other guests were tested by UV and fluorescence titrations.^{49,50} Scheme 11 shows guest molecules that were found to form 1:1 complexes with

(48) Fluorescence spectra of the Zn^{2+} complexes **6** and **8** showed negligible change upon addition of anions such as OH^- , carboxylates, phosphates, imides, and thiolates at neutral pH, due to strong binding of the side chain to Zn^{2+} .

(49) For reviews of anion receptors and sensors, see: (a) Lehn, J.-M. *Supramolecular Chemistry: Concepts and Perspectives*; VCH: Weinheim, Germany, 1995. (b) *Supramolecular Chemistry of Anions*; Bianchi, A., Bowman-James, K., Garcia-Espana, E., Eds.; Wiley-VCH: New York, 1996. (c) Sessler, J. L.; Andrievsky, A.; Genge, J. W. In *Advances in Supramolecular Chemistry*, Vol. 4.; Gokel, G. W., Ed.; JAI Press Inc.: Greenwich, CT, 1997; pp 97–142. (d) Seel, C.; Galán, A.; de Mendoza, J. *Top. Curr. Chem.* **1995**, *175*, 101–132. (e) Scheerder, J.; Engbersen, J. F. J.; Reinhoudt, D. N. *Recl. Trav. Chim. Pays-Bas* **1996**, *115*, 307–320. (f) Beer, P. D. *J. Chem. Soc., Chem. Commun.* **1996**, 689–696. (g) de Silva, A. P.; Nimal Gunaratne, H. Q.; Gunlaugsson, T.; Huxley, A. J. M.; McCoy, C. P.; Rademacher, J. T.; Rice, T. E. *Chem. Rev.* **1997**, *97*, 1515–1566. (h) Schmidtchen, F. P.; Berger, M. *Chem. Rev.* **1997**, *97*, 1609–1646. (i) Hamilton, A. D. *Chem. Rev.* **1997**, *97*, 1609–1646. (j) Beer, P. D. *Acc. Chem. Res.* **1998**, *31*, 71–80. (k) Beer, P. D.; Cadman, J. *Coord. Chem. Rev.* **2000**, *205*, 131–155. (l) Beer, P. D.; Gale, P. A. *Angew. Chem., Int. Ed.* **2001**, *40*, 487–516. (m) Wiskur, S. L.; Ait-Haddou, H.; Ansllyn, E. V.; Lavigne, J. J. *Acc. Chem. Res.* **2001**, *34*, 963–972.

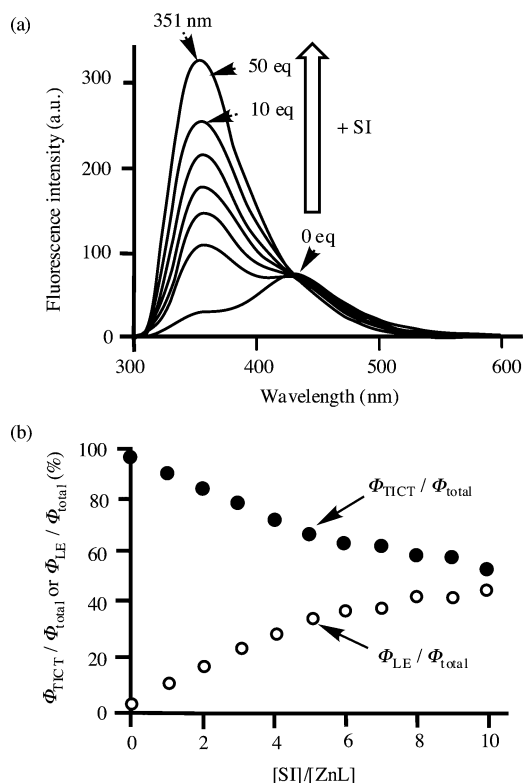


Figure 11. (a) Change in fluorescence spectra of ZnL6 (0.2 mM) upon addition of succinimide (SI) (0–50 equiv) at pH 7.0 (10 mM HEPES with $I = 0.1$ (NaNO_3)) and 25 °C (excitation at 270 nm). (b) Distribution of $\Phi_{\text{TICT}}/\Phi_{\text{total}}$ and $\Phi_{\text{LE}}/\Phi_{\text{total}}$ of ZnL6 upon addition of SI at pH 7.0 (10 mM HEPES with $I = 0.1$ (NaNO_3)) and 25 °C (excitation at 270 nm) ($\Phi_{\text{LE}}/\Phi_{\text{total}}$, open circles; $\Phi_{\text{TICT}}/\Phi_{\text{total}}$, solid circles).

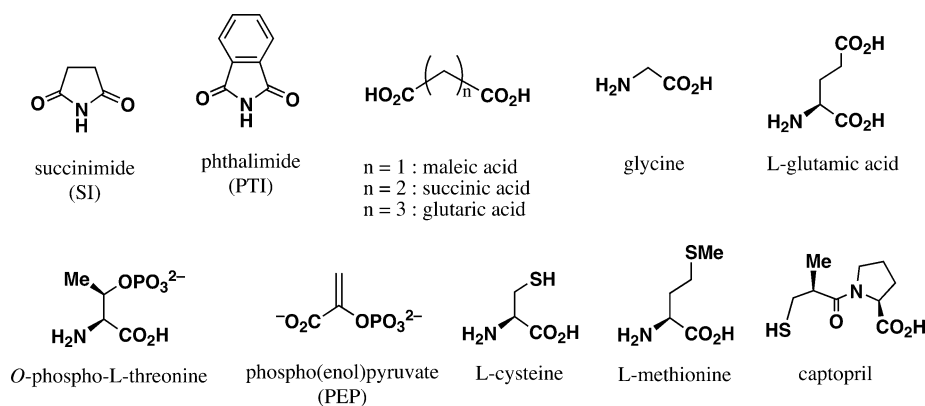
ZnL6 in D_2O at pH 7.0 and 25 °C by ^1H NMR experiments.⁵¹ Figure 12 displays the fluorescence response of ZnL6 (0.2 mM) at 355 nm (LE emission) against these anions at pH 7.0 (10 mM HEPES with $I = 0.1$ (NaNO_3)) and 25 °C. The $\log K_{\text{app}}(\text{ZnL6-X}^-)$ values for these anions are listed in Table 2.

Despite a negligible response against monocarboxylic acids such as acetic acid (curve e in Figure 12) and glycine, the enhancement of LE emission was observed upon addition of a diacid such as malonic acid, succinic acid, and glutaric acid (curve d), suggesting that two carboxylates cooperatively bind to Zn^{2+} of ZnL6. Phosphates such as HOPO_3^{2-} (curve b), *O*-phospho-L-threonine, and phospho(enol)pyruvate, and thiols

(50) For recent examples of anion sensors in aqueous solution, see: (a) Anzenbacher, P., Jr.; Try, A. C.; Miyaji, H.; Jursazkova, K.; Lynch, V. M.; Marquez, M.; Sessler, J. L. *J. Am. Chem. Soc.* **2000**, *122*, 10268–10272. (b) Amendola, V.; Basteianello, E.; Fabbri, L.; Mangano, C.; Pallavicini, P.; Perotti, A.; Lanfredi, A. M.; Ugozzoli, F. *Angew. Chem., Int. Ed.* **2000**, *39*, 2917–2920. (c) Schneider, S. E.; O’Neil, S. N.; Ansllyn, E. V. *J. Am. Chem. Soc.* **2000**, *122*, 542–543. (d) Choi, K.; Hamilton, A. D. *J. Am. Chem. Soc.* **2001**, *123*, 2456–2457. (e) Wiskur, S. L.; Ansllyn, E. V. *J. Am. Chem. Soc.* **2001**, *123*, 10109–10110. (f) Cabell, L. A.; Best, M. D.; Lavigne, J. J.; Schneider, S. E.; Perreault, D. M.; Monahan, M.-K.; Ansllyn, E. V. *J. Chem. Soc., Perkin Trans. 2* **2001**, 315–323. (g) Dickins, R. S.; Aime, S.; Batsanov, A. S.; Beeby, A.; Botta, M.; Bruce, J. I.; Howard, J. A. K.; Love, C. S.; Parker, D.; Peacock, R. D.; Puschmann, H. *J. Am. Chem. Soc.* **2002**, *124*, 12697–12705. (h) Mizukami, S.; Nagano, T.; Urano, Y.; Odani, A.; Kikuchi, K. *J. Am. Chem. Soc.* **2002**, *124*, 3920–3925. (i) Ojida, A.; Mito-oka, Y.; Inoue, M.; Hamachi, I. *J. Am. Chem. Soc.* **2002**, *124*, 6256–6258. (j) Rekharsky, M.; Inoue, Y.; Tobey, S.; Metzger, A.; Ansllyn, E. V. *J. Am. Chem. Soc.* **2002**, *124*, 14959–14967. (k) Tobey, S. L.; Ansllyn, E. V. *J. Am. Chem. Soc.* **2003**, *125*, 14807–14815.

(51) By Job plots (^1H NMR) with anions (Figure S10 in the Supporting Information), ZnL6 forms 1:1 complexes with malonic acid, glutaric acid, captopril, phosphate (HOPO_3^{2-}), and phospho(enol)pyruvate. It was suggested that PPI yields a 1:2 ZnL6-PPI complex and citric acid gives a mixture of 1:2 and 1:3 complexes with ZnL6.

Scheme 11



such as captopril (curve c), L-cysteine, and L-cysteine methyl ester, induced remarkable increases in LE emission (Figure 12).^{52,53} A negligible response against L-methionine (curve f) suggests that thiolates strongly bind to Zn²⁺. No relationship was found between $K_{\text{app}}(\text{ZnL6-X}^-)$ values and emission enhancement. We consider that emission intensities are affected by not only basicities and steric hindrance of guest molecules but also kinetic inertness of ZnL6-X⁻ complexes. Halide anions (F⁻, Cl⁻, Br⁻, and I⁻) and CO₃²⁻ (up to 10 equiv) caused negligible changes of the emission spectra of ZnL6 in aqueous solution.^{54,55}

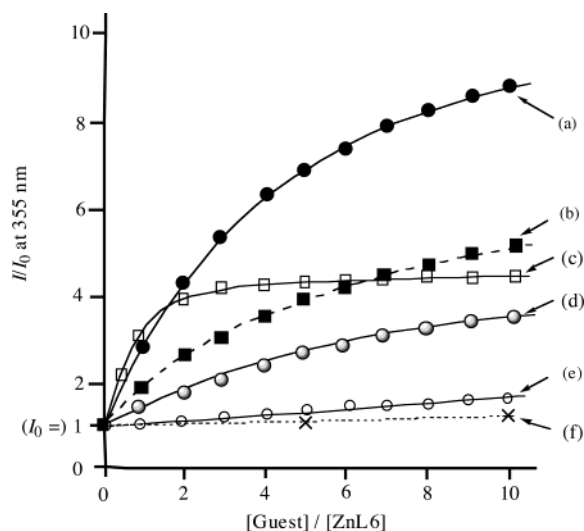


Figure 12. Fluorescence response of ZnL6 (0.2 mM) at 355 nm (excitation at 265 nm) against succinimide (a), inorganic phosphate (HPO₄²⁻) (b), captopril (c), malonic acid (d), acetic acid or L-methionine (e), and halide anions (F⁻, Cl⁻, Br⁻, or I⁻) (f) at pH 7.0 (10 mM HEPES with $I = 0.1$ (NaNO₃)) and 25 °C. I_0 is the emission intensity of ZnL6 at 355 nm in the absence of a guest.

X-ray Crystal Structure of ZnL6–Phthalimidate Complex 22.

Fine colorless crystals were isolated from a mixture of ZnL6

- (52) The ¹H NMR experiments confirmed that ZnL6 does not decompose upon addition of SI, phosphates, and thiolates.
- (53) The ¹H NMR experiments suggested that ZnL6 forms a 1:1 complex with maleic acid (cis) and a 1:2 complex with fumaric acid (trans). The UV and fluorescence titrations of ZnL6 with maleic acid and fumaric acid gave unclear results, because these diacids have a UV absorption at ca. 280 nm.
- (54) In CH₃CN, acetate, F⁻, Cl⁻, and Br⁻ induce the emission change of ZnL6 (0.2 mM) from TICT to LE (these anions were added as Bu₄N⁺ or Et₄N⁺ salts). The log $K_{\text{app}}(\text{ZnL6-X}^-)$ values were 2.7 ± 0.1 for AcO⁻, 2.0 ± 0.2 for F⁻, 2.1 ± 0.1 for Cl⁻, and 2.0 ± 0.1 for Br⁻ (Figure S11 in the Supporting Information). On the other hand, I⁻ quenched the emissions of ZnL6 (log $K_{\text{app}}(\text{ZnL6-I}^-)$ was 3.5 ± 0.1). An addition of HPO₄²⁻·Bu₄N⁺ to ZnL6 (0.2 mM) in CH₃CN caused colorless precipitations.

Table 2. Complexation Constants of Zn²⁺ Complexes 5 and 13 with Guest Anions

guest (pK _a ^a)	5 (Zn ²⁺ -cyclen) log K_{app} at pH 7.0 ^b	13 (ZnL6) log K_{app} at pH 7.0 ^b
acetic acid (4.73)	1.8 ^c	1.9 ^d
malonic acid (<3, 5.43)	nd ^e	2.5, ^d 2.6 ^f
succinic acid (4.12, 5.37)	nd ^e	2.6, ^d 2.6 ^f
glutaric acid (4.27, 5.11)	nd ^e	2.5, ^d 2.6 ^f
L-glutamic acid (<3, 4.29, 9.73) ^g	nd ^e	2.1 ^f
succinimide (9.61)	3.0 ^d	2.7, ^d 2.8, ^f 3.1 ^g
L-cysteine (<3, 8.23, 10.33) ^g	nd ^e	4.3, ^d 4.4 ^f
L-cysteine methyl ester (nd ^e)	nd ^e	4.2, ^d 4.3 ^f
L-methionine (nd ^e)	nd ^e	<1.5 ^f
captopril (3.58, 9.97) ^g	4.1 ^h	4.0, ^d 4.1 ^f
phosphate (<3, 6.92, >11)	3.3 ^h	2.8, ^d 2.9, ^f 2.7 ^g
pyrophosphate (<3, <3, 6.10, 8.27)	nd ^e	1:2 complexation ⁱ
phospho(enol)pyruvate (<3, 3.47, 6.16)	nd ^e	3.7 ^f
O-phospho-L-threonine (<3, <3, 6.08, 9.96)	nd ^e	2.7, ^d 2.8 ^f

^a pK_a values were determined by potentiometric pH titrations at 25 °C with $I = 0.1$ (NaNO₃). Experimental errors are ±0.05. ^b For definition, see the text. ^c From ref 15 at 25 °C with $I = 0.1$ (NaNO₃). ^d Determined by UV titrations at [ZnL6] = 0.2 mM. ^e nd = not determined. ^f Determined by fluorometric titrations at [ZnL6] = 0.2 mM. ^g Determined by potentiometric pH titration. ^h From ref 11 at 25 °C with $I = 0.1$ (NaNO₃). ⁱ Confirmed by Job plots in the ¹H NMR experiments (Figure S10 in the Supporting Information).

and phthalimide (PTI) in aqueous solution at pH 6.5. The X-ray crystal structure analysis has proven the 1:1 complexation of ZnL6 and deprotonated PTI (PTI⁻). As shown in Figure 13, the 1:1 ZnL6–PTI⁻ complex (**22**) is stabilized by coordination of deprotonated imide nitrogen to Zn²⁺ (Zn²⁺–N(21) = 1.95 Å) and the hydrogen bonds between the carbonyl oxygen of PTI⁻ and cyclen NH (the distances between O(PTI) and the amino protons are 2.22 and 2.86 Å). The dihedral angle for C(13)–N(2)–C(14)–N(15) of 7.0° indicates the planar conformation of the pyridine ring of ZnL6 with respect to the dialkylamino group. A pyridine ring of ZnL6 and a phenyl ring of PTI are fixed in a parallel fashion: the distance between

- (55) The response of CdL6 (prepared in situ at [Cd]_{total} = [L6]_{total} = 0.2 mM) against phosphates and SI was smaller than that of ZnL6 (Figure S12 in the Supporting Information). The log $K_{\text{app}}(\text{CdL6-SI}^-)$ value was calculated to be <2. An addition of pyrophosphate to CdL6 (0.2 mM) in 10 mM HEPES (pH 7.0 with $I = 0.1$ (NaNO₃)) at 25 °C caused an increase of LE emission, due to the decomplexation of CdL6, as judged by ¹H NMR and UV experiments. These results are interesting in comparison with the Cd²⁺ complex developed by Nagano et al., which was reported to be a phosphate sensor in aqueous solution (ref 50h).

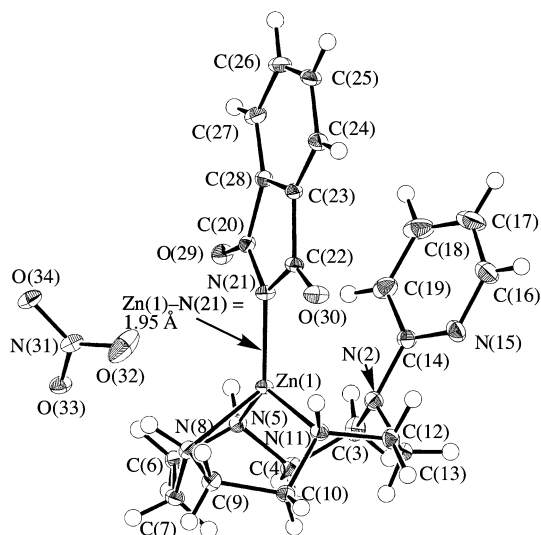
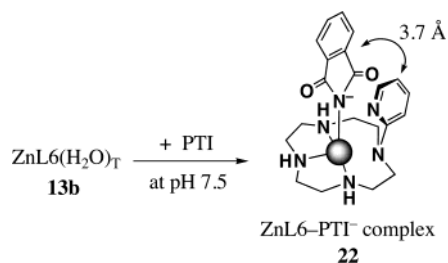


Figure 13. ORTEP drawing (50% probability ellipsoids) of ZnL6–phthalimidate (ZnL6–PTI[−]) complex (**22**). Selected bond distances (Å): Zn(1)–N(2) 2.494(1), Zn(1)–N(5) 2.067(1), Zn(1)–N(8) 2.132(1), Zn(1)–N(11) 2.089(1), Zn(1)–N(21) 1.954(1), Zn(1)–O(48) 2.302(1), N(2)–C(14) 1.421(2), C(14)–N(15) 1.332(2). Selected dihedral angles (deg): C(3)–N(2)–C(14)–N(15) −140.4°, C(3)–N(2)–C(14)–C(19) 43.3°, C(13)–N(2)–C(14)–N(15) −7.0°, C(13)–N(2)–C(14)–C(19) 176.7°.

Scheme 12



these two rings is ca. 3.7 Å, suggesting a π – π stacking interaction (Scheme 12).⁵⁶

¹H NMR Studies of ZnL6 and ZnL6–Anion Complexes. The ¹H NMR spectra of phosphate, SI[−], and PTI[−] complexes of ZnL6 in aqueous solution at pD 7.4 and 25 °C were obtained. Figure 14a shows the ¹H NMR spectra (aromatic regions) of ZnL6 at pD 7.4 and 35 °C. A nuclear Overhauser effect (NOE) was observed (ca. 3%) between H(19) and the axial proton on C(4) (H(4)_{ax}, see Figure 7 for the numbering) adjacent to the pyridyl amino group, implying the twisted conformation in **13b** (ZnL6(H₂O)₇) (Scheme 13). At pD 11.0, upfield shifts of the H(3'), H(4'), and H(5') signals and downfield shifts of the H(4)_{ax} peaks were observed (Figure 14b), possibly due to the partial release of twisted conformation. The NOE effect between H(19) and H(4)_{ax} was not clearly observed for the ZnL6–phosphate complex **23**, because the ¹H signal of H(4)_{ax} shifts downfield and signals of other cyclen protons are overlapped (Figure 14c). The ¹H NMR spectra of ZnL6 at pD 7.0 in the presence of phosphate (10 equiv), SI (10 equiv), and PTI (1 equiv) in Figure 14c–e showed similar behaviors, supporting that complexation with these guests induces conformational change. Larger upfield shifts of aromatic protons of ZnL6 in **22** are attributed to the shielding effects of the aromatic ring of PTI (Figure 14e).

(56) We could not determine the $\log K_{\text{app}}(\text{ZnL}^{\text{L}}\text{--PTI}^{\text{L}})$ value by UV and fluorescent titrations due to the overlap of UV absorptions of ZnL6 and PTI.

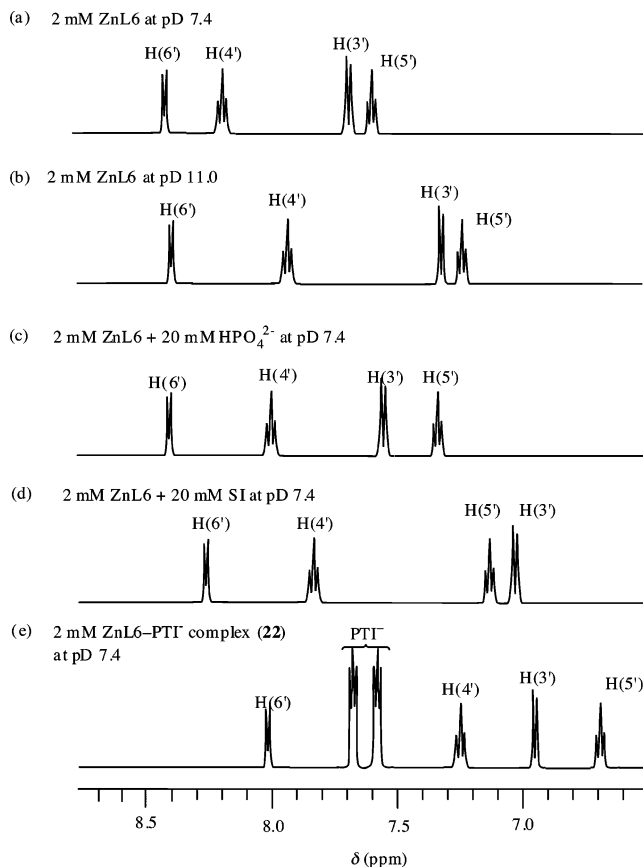


Figure 14. ¹H NMR spectra (aromatic region) of 2 mM ZnL6 at pD 7.4 (a), 2 mM ZnL6 at pD 11.0 (b), 2 mM ZnL6 + 20 mM phosphate at pD 7.4 (c), 2 mM ZnL6 + 20 mM SI (d), and 2 mM ZnL6–PTI[−] complex (**22**) at pD 7.4 (e) in D₂O at 25 °C.

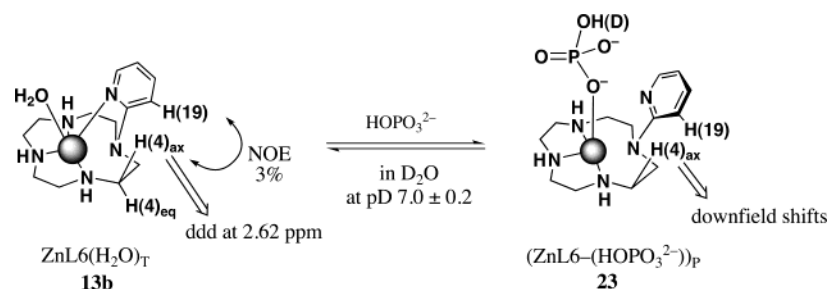
Interestingly, the ¹H NMR spectra of a 2:1 mixture of ZnL6 (3 mM) and captopril (1.5 mM)⁵⁷ exhibited two independent sets of peaks for the aromatic protons of ZnL6 in a 1:1 ratio, corresponding to free ZnL6 and the 1:1 ZnL6–captopril complex (see Figure S13 in the Supporting Information). In contrast, a 2:1 mixture of ZnL6 (3 mM) and glutaric acid (1.5 mM) showed gradual upfield shifts of aromatic proton signals of ZnL6, which were thus averaged peaks of uncomplexed ZnL6 and complexed species of ZnL6. These phenomena suggest that the ZnL6–captopril complex is not only thermodynamically stable at millimolar order but also kinetically inert on the NMR time scale (400 and 500 MHz).

Conclusion

We have synthesized *N*-(2-(5-cyanopyridyl))cyclen **10** (**L5**) and *N*-(2-pyridyl)cyclen **11** (**L6**) in order to control TICT in aqueous solution utilizing the potent binding properties of cyclen. In particular, **11** (**L6**) is a unique ligand which exhibits TICT emission due to formation of stable complexes with Zn²⁺ and Cd²⁺. This is the first successful example of metal chelation control of TICT and should give clear evidence for an anomalous emission at longer wavelengths from a twisted conformer.

(57) It is reported that captopril has two conformers, trans and cis, with respect to the amide bond: (a) Rabenstein, D. L.; Isab, A. A. *Anal. Chem.* **1982**, *54*, 526–529. (b) Hughes, M. A.; Smith, G. L.; Williams, D. R. *Inorg. Chim. Acta* **1985**, *107*, 247–252. (c) Isab, A. A.; Hussain, M. S. *Can. J. Anal. Sci. Spectrosc.* **1997**, *42*, 102–106. The ¹H NMR experiments suggested that both conformers bind to ZnL6 (Figure S13 in the Supporting Information).

Scheme 13



Moreover, ZnL6 forms complexes with external anions such as imidates, phosphates, thiolates, and dicarboxylates, resulting in fluorescence emission at shorter wavelengths by release of a twisted conformation of the pyridine ring. The CdL6 complex (prepared in situ) was not as sensitive to guest anions as ZnL6.⁵⁵ The Zn^{2+} ion is more favorable as a center metal for anion sensors because it offers several advantages: (i) Zn^{2+} is a strong Lewis acid and binds strongly with anions, (ii) Zn^{2+} does not absorb UV and visible lights, and (iii) the coordination number of the Zn^{2+} ion is rather flexible between 4 and 6. The energy difference between four- and six-coordinated Zn^{2+} ions has been estimated to be only about 0.4 kcal/mol.⁵⁸

Most previous fluorescence sensing mechanisms for sensors of metals or anions include PET, fluorescence resonance energy transfer (FRET), or charge transfers (CT). Chelation-controlled

TICT with a considerable shift of emission wavelength may provide new methodologies for designing novel fluorescence sensors for metal ions and biologically relevant anions in aqueous solution.

Acknowledgment. E.K. and S.A. are thankful for the Grants-in-Aid from the Ministry of Education, Science and Culture in Japan (Nos. 12771355, 13557195, and 15590008). S.A. acknowledges the grants from the Mitsubishi Chemical Corp. Fund (Tokyo), Toray Science Foundation (Chiba), and Terumo Life Science Foundation (Kanagawa). We thank NMR instruments (for the JEOL Alpha (400 MHz)) in the Research Center for Molecular Medicine (RCMM) at Hiroshima University.

Supporting Information Available: Figures S1–S11, and tables and CIF data for **11** (L6), **13** (ZnL6), and the **13**–PTI[−] (ZnL6-(PTI[−])) complex (**22**) (PDF, CIF). This material is available free of charge via the Internet at <http://pubs.acs.org>.

JA040095V

(58) (a) Vallee, B. L.; Auld, D. S. In *Interface between Chemistry and Biochemistry*; Jolles, P., Jörnvall, H., Eds.; Birkhäuser Verlag: Basel, 1995; pp 259–277. (b) Lipscomb, W. N.; Sträter, N. *Chem. Rev.* **1996**, *96*, 2375–2433.